

Anatomy of Vector-Like Top-Quark Models in the Alignment Limit of the 2-Higgs Doublet Model Type-II

A. ARHRIB^{1*}, R. BENBRIK^{2†}, M. BOUKIDI^{2‡}, B. MANAUT^{3§}, S. MORETTI^{4,5¶}

¹*Abdelmalek Essaadi University, Faculty of Sciences and Techniques, Tangier, Morocco*

²*Polydisciplinary Faculty, Laboratory of Fundamental and Applied Physics, Cadi Ayyad University, Sidi Bouzid, B.P. 4162, Safi, Morocco*

³*Polydisciplinary Faculty, Laboratory of Research in Physics and Engineering Sciences, Sultan Moulay Slimane University, Beni Mellal 23000, Morocco*

⁴*Department of Physics & Astronomy, Uppsala University, Box 516, SE-751 20 Uppsala, Sweden*

⁵*School of Physics & Astronomy, University of Southampton, Southampton, SO17 1BJ, United Kingdom*

Abstract

A comprehensive extension of the ordinary 2-Higgs Doublet Model (2HDM), supplemented by Vector-Like Quarks (VLQs), in the “alignment limit” is presented. In such a scenario, we study the possibility that Large Hadron Collider (LHC) searches for VLQs can profile their nature too, i.e., whether they belong to a singlet, doublet, or triplet representation. To achieve this, we exploit both Standard Model (SM) decays of VLQs with top-(anti)quark Electromagnetic (EM) charge (T), i.e., into b, t quarks and W^\pm, Z, h bosons (which turn out to be suppressed and hence T states can escape existing limits) as well as their exotic decays, i.e., into b, t (and possibly B) quarks and H^\pm, H, A bosons. We show that quite specific decay patterns emerge in the different VLQ representations so that, depending upon which T signals are accessed at the LHC, one may be able to ascertain the underlying Beyond Standard Model (BSM) structure, especially if mass knowledge of the new fermionic and bosonic sectors can be inferred from (other) data.

*aarhrib@gmail.com

†r.benbrik@uca.ac.ma

‡mohammed.boukidi@ced.uca.ma

§b.manaut@usms.ma

¶stefano.moretti@physics.uu.se; s.moretti@soton.ac.uk

1 Introduction

Following the discovery of a Higgs boson, h , during Run 1 of the Large Hadron Collider (LHC) at CERN [1, 2], the ATLAS and CMS collaborations have carried out a broad programme of measurements of its properties, namely, mass, spin, CP quantum numbers, etc. These all seem to point to a Standard Model (SM) nature of such a new state. However, some anomalies exist in current data that may point to a Beyond the SM (BSM) framework accommodating such a discovery. The signal strength of the $t\bar{t}h$ associated production mode is one of those most prominent, while milder effects are still seen in the fits to data when assuming the gluon-gluon fusion production mode, especially when combined with di-photon decays. Further, current measurements of the $h \rightarrow \gamma Z$ decay channel do not exclude that its rate can differ from SM predictions. A possibility to capture at once all such anomalies is offered by the presence of Vector-Like Quarks (VLQs) as they could affect simultaneously the one-loop induced (chiefly by t quarks) SM-like Higgs production and decay channels as well as mediate a $t\bar{t}h$ final state.

At the same time, having established the doublet nature of the SM-like Higgs field so far discovered, much experimental attention has lately been aroused by the possibility that other Higgs doublets could exist in nature. The simplest option is the one offered by a 2-Higgs Doublet Model (2HDM) [3]. Herein, four additional Higgs bosons exist: a heavier CP-even state, H , a CP-odd one, A , and a pair of charged ones, H^\pm . All such new Higgs states could then manifest themselves at the LHC in new direct signals, i.e., when they are produced as resonant objects inside the detectors, or else indirectly, e.g., via loop effects in a variety of single and double h production modes. In fact, in the first case, they may well be produced in the decays of new particles.

Therefore, it is intriguing to study models that embed 2HDM (pseudo)scalar states as well as VLQs. Indeed, we concentrate here on both these states at once. While the nature of the former has already been described, it is worth reminding the reader that the latter are heavy spin 1/2 particles that transform as triplets under colour but, unlike SM quarks, their left- and right-handed couplings have the same Electroweak (EW) quantum numbers. Furthermore, their couplings to Higgs bosons do not participate in the standard EW Symmetry Breaking (EWSB) dynamics onset by the Higgs mechanism, hence, they are not of Yukawa type (i.e., proportional to the mass), rather they are additional parameters, which can then be set as needed in order to achieve both compliance with present data and predict testable signals for the future.

Amongst the ensuing signatures, an exciting possibility is constituted by the decays of VLQs into the additional Higgs states of a 2HDM, which are not currently being pursued at the LHC. (Recently, we have advocated that $\gamma\gamma$ and $Z\gamma$ signatures of a heavy neutral Higgs state produced from a heavy VLQ top state might be accessible during Run 3 [4].) The ATLAS and CMS collaborations, while collecting data at 7, 8, and 13 TeV, have performed searches for VLQs with different quantum numbers, probing single and pair production mechanisms but limited to decay modes into SM quarks and gauge/Higgs bosons (for the most updated experimental results of ATLAS and CMS, we refer to the respective web pages [5–7]). However, no evidence for the existence of other quarks, besides those of the SM, has been obtained. The reason may indeed be that additional fermions may preferentially decay into additional Higgs states, rather than via SM objects.

Another motivation for pursuing the phenomenological exploitation of a 2HDM plus VLQs (henceforth, ‘2HDM+VLQ’) construct finally comes from the expectation that, by leveraging

the cancellations that may occur at the loop level between the bosonic (onset by the additional Higgs states) and fermionic (onset by the additional VLQ states) contributions, as well as the altered coupling structure of the SM states (chiefly, of the SM-like Higgs and third generation quarks), a larger expanse of parameter space of this model will be compatible with EW Precision Observables (EWPOs), from LEP and SLC, than what would be released by only accounting for separate (as opposed to simultaneous) effects from, on the one hand, 2HDM Higgses or, on the other hand, VLQs. Indeed, it would be rewarding to verify that this can happen for rather light masses of both additional Higgs and VLQ states so that they can both be searched for at the LHC shortly through the aforementioned exotic decays.

In the present paper, we wish to build on the results of [8–24], but especially [4], by studying a 2HDM plus VLQ scenario where the VLQs can belong to a singlet, doublet, or triplet representation under the SM gauge group $SU(3)_C \times SU(2)_L \times U(1)_Y$. We intend to tension the scope afforded, in the quest for such VLQs, by their exotic decays (involving the additional Higgs states of the 2HDM, both neutral and charged, as well as other, lighter VLQs) against the one already established through their SM decays, involving standard quarks and gauge/Higgs bosons as final state products. Particularly, we will pursue the task of uniquely attributing certain VLQ decay patterns into exotic states that may be established at the LHC to one or another of the three aforementioned multiplet structures.

Our paper is organised as follows. In the next section, we describe in some detail the three theoretical structures concerned, both their model construction and implementation. In Sect. III, using three subsections, one for each multiplet realization, we present our results. All this is followed by our conclusions, in Sect. IV. We also have an Appendix with relevant Feynman rules involving Higgs states and the new VLQs.

2 Model description

2.1 Formalism

In this paper, we extend Ref. [9], wherein a CP-conserving 2HDM with a singlet VLQ companion to the (chiral) top quark of the SM was set up, that contained the canonical Higgs states: as mentioned, two CP-even states denoted by h (the lightest) and H (the heaviest), one CP-odd state denoted by A and two charged states denoted by H^\pm . As tree-level Flavour Changing Neutral Currents (FCNCs) are very constrained by experiment, we imposed a \mathbb{Z}_2 symmetry, $\Phi_1 \rightarrow \Phi_1$ and $\Phi_2 \rightarrow -\Phi_2$, on the Higgs fields. The resulting Higgs potential (softly broken by the dimension two terms $\propto m_{12}^2$) can be written as

$$\begin{aligned} \mathcal{V} = & m_{11}^2 \Phi_1^\dagger \Phi_1 + m_{22}^2 \Phi_2^\dagger \Phi_2 - \left(m_{12}^2 \Phi_1^\dagger \Phi_2 + \text{h.c.} \right) + \frac{1}{2} \lambda_1 \left(\Phi_1^\dagger \Phi_1 \right)^2 + \frac{1}{2} \lambda_2 \left(\Phi_2^\dagger \Phi_2 \right)^2 \\ & + \lambda_3 \Phi_1^\dagger \Phi_1 \Phi_2^\dagger \Phi_2 + \lambda_4 \Phi_1^\dagger \Phi_2 \Phi_2^\dagger \Phi_1 + \left[\frac{1}{2} \lambda_5 \left(\Phi_1^\dagger \Phi_2 \right)^2 + \text{h.c.} \right]. \end{aligned} \quad (1)$$

choosing real Vacuum Expectation Values (VEVs) for the two Higgs doublet fields, v_1 and v_2 , and demanding m_{12}^2 and λ_5 to be real, the potential is indeed CP-conserving. The free independent parameters are here taken to be the four masses, m_h , m_H , m_A and m_{H^\pm} , the soft breaking parameter m_{12} , the VEV ratio $\tan \beta = v_2/v_1$ and the mixing term $\sin(\beta - \alpha)$, where the angle α diagonalizes the CP-even mass matrix. When we impose that no (significant) tree-level FCNCs are present in the theory using the (softly broken) \mathbb{Z}_2 symmetry, we end up

with four different Yukawa versions of the model. These are Type-I, where only Φ_2 couples to all fermions; Type-II, where Φ_2 couples to up-type quarks and Φ_1 couples to charged leptons and down-type quarks; Type-Y (or Flipped), where Φ_2 couples to charged leptons and up-type quarks and Φ_1 couples to down-type quarks; Type-X (or Lepton Specific), where Φ_2 couples to quarks and Φ_1 couples to charged leptons¹.

The gauge invariant structures that have multiplets with definite $SU(3)_C \times SU(2)_L \times U(1)_Y$ quantum numbers appear in the interactions of new VLQs with the SM states via renormalizable couplings. The set of VLQ representations is indicated by:

$$\begin{aligned} T_{L,R}^0 & && (\text{singlets}), \\ (X T^0)_{L,R}, \quad (T^0 B^0)_{L,R} & && (\text{doublets}), \\ (X T^0 B^0)_{L,R}, \quad (T^0 B^0 Y)_{L,R} & && (\text{triplets}). \end{aligned} \quad (2)$$

We use in this section a zero superscript to distinguish the weak eigenstates from the mass eigenstates. The electric charges of the new VLQs are $Q_T = 2/3$, $Q_B = -1/3$, $Q_X = 5/3$ and $Q_Y = -4/3$. Note that T and B carry the same electric charge as the SM top and bottom quarks, respectively.

The physical up-type quark mass eigenstates may, in general, contain non-zero $Q_{L,R}^0$ (with Q being the VLQ field) components, when new fields $T_{L,R}^0$ of charge $2/3$ and non-standard isospin assignments are added to the SM. This situation leads to a deviation in their couplings to the Z boson. Atomic parity violation experiments and the measurement of R_c at LEP give some constraints on these deviations for the up and charm quarks which are far stronger than for the top quark. In the Higgs basis, the Yukawa Lagrangian contains the following terms:

$$-\mathcal{L} \supset y^u \bar{Q}_L^0 \tilde{H}_2 u_R^0 + y^d \bar{Q}_L^0 H_1 d_R^0 + M_u^0 \bar{u}_L^0 u_R^0 + M_d^0 \bar{d}_L^0 d_R^0 + \text{h.c.} \quad (3)$$

Here, u_R actually runs over (u_R, c_R, t_R, T_R) and d_R actually runs over (d_R, s_R, b_R, B_R) .

We now turn to the mixing of the new partners to the third generation, y_u and y_d , which are 3×4 Yukawa matrices. In fact, in the light of the above constraints, it is very reasonable to assume that only the top quark t ‘‘mixes’’ with T . In this case, the 2×2 unitary matrices $U_{L,R}^u$ define the relation between the charge $2/3$ weak and mass eigenstates:

$$\begin{pmatrix} t_{L,R} \\ T_{L,R} \end{pmatrix} = U_{L,R}^u \begin{pmatrix} t_{L,R}^0 \\ T_{L,R}^0 \end{pmatrix} = \begin{pmatrix} \cos \theta_{L,R}^u & -\sin \theta_{L,R}^u e^{i\phi_u} \\ \sin \theta_{L,R}^u e^{-i\phi_u} & \cos \theta_{L,R}^u \end{pmatrix} \begin{pmatrix} t_{L,R}^0 \\ T_{L,R}^0 \end{pmatrix}. \quad (4)$$

In contrast to the up-type quark sector, the addition of new fields $B_{L,R}^0$ of charge $-1/3$ in the down-type quark sector results in four mass eigenstates d, s, b, B . Measurements of R_b at LEP set constraints on the b mixing with the new fields that are stronger than for mixing with the lighter quarks d, s . In this case, then, 2×2 unitary matrices $U_{L,R}^d$ define the dominant $b - B$ mixing as

$$\begin{pmatrix} b_{L,R} \\ B_{L,R} \end{pmatrix} = U_{L,R}^d \begin{pmatrix} b_{L,R}^0 \\ B_{L,R}^0 \end{pmatrix} = \begin{pmatrix} \cos \theta_{L,R}^d & -\sin \theta_{L,R}^d e^{i\phi_d} \\ \sin \theta_{L,R}^d e^{-i\phi_d} & \cos \theta_{L,R}^d \end{pmatrix} \begin{pmatrix} b_{L,R}^0 \\ B_{L,R}^0 \end{pmatrix}. \quad (5)$$

(More details on this Lagrangian formalism are shown in the Appendix.) To ease the notation, we have dropped the superscripts $u(d)$ whenever the mixing occurs only in the up(down)-type quark sector. Additionally, we sometime use the shorthand notations $s_{L,R}^{u,d} \equiv \sin \theta_{L,R}^{u,d}$, $c_{L,R}^{u,d} \equiv \cos \theta_{L,R}^{u,d}$, etc.

This Lagrangian contains all the phenomenological relevant information:

¹In this paper, we will be discussing only Type-II.

- (i) the modifications of the SM couplings that might show indirect effects of new quarks can be found in the terms that do not contain heavy quark fields;
- (ii) the terms relevant for LHC phenomenology (i.e., heavy quark production and decay) are those involving a heavy and a light quark;
- (iii) terms with two heavy quarks are relevant for their contribution to oblique corrections.

In the weak eigenstate basis, the diagonalization of the mass matrices makes the Lagrangian of the third generation and heavy quark mass terms such as

$$\begin{aligned} \mathcal{L}_{\text{mass}} = & - (\bar{t}_L^0 \quad \bar{T}_L^0) \begin{pmatrix} y_{33}^u \frac{v}{\sqrt{2}} & y_{34}^u \frac{v}{\sqrt{2}} \\ y_{43}^u \frac{v}{\sqrt{2}} & M^0 \end{pmatrix} \begin{pmatrix} t_R^0 \\ T_R^0 \end{pmatrix} \\ & - (\bar{b}_L^0 \quad \bar{B}_L^0) \begin{pmatrix} y_{33}^d \frac{v}{\sqrt{2}} & y_{34}^d \frac{v}{\sqrt{2}} \\ y_{43}^d \frac{v}{\sqrt{2}} & M^0 \end{pmatrix} \begin{pmatrix} b_R^0 \\ B_R^0 \end{pmatrix} + \text{h.c.}, \end{aligned} \quad (6)$$

with M^0 a bare mass term², y_{ij}^q , $q = u, d$, Yukawa couplings and $v = 246$ GeV the Higgs VEV in the SM. Using the standard techniques of diagonalization, the mixing matrices are obtained by

$$U_L^q \mathcal{M}^q (U_R^q)^\dagger = \mathcal{M}_{\text{diag}}^q, \quad (7)$$

with \mathcal{M}^q the two mass matrices in Eq. (6) and $\mathcal{M}_{\text{diag}}^q$ the diagonals ones. To check the consistency of our calculation, the corresponding 2×2 mass matrix reduces to the SM quark mass term if either the T or B quarks are absent.

Notice also that, in multiplets with both T and B quarks, the bare mass term is the same for the up- and down-type quark sectors. For singlets and triplets one has, $y_{43}^q = 0$ whereas for doublets $y_{34}^q = 0$. Moreover, for the (XTB) triplet one has $y_{34}^d = \sqrt{2}y_{34}^u$ and for the (TBY) triplet one has $y_{34}^u = \sqrt{2}y_{34}^d$ ³.

The mixing angles in the left- and right-handed sectors are not independent parameters. From the mass matrix bi-unitary diagonalization in Eq. (7) one finds:

$$\begin{aligned} \tan 2\theta_L^q &= \frac{\sqrt{2}|y_{34}^q|vM^0}{(M^0)^2 - |y_{33}^q|^2v^2/2 - |y_{34}^q|^2v^2/2} \quad (\text{singlets, triplets}), \\ \tan 2\theta_R^q &= \frac{\sqrt{2}|y_{43}^q|vM^0}{(M^0)^2 - |y_{33}^q|^2v^2/2 - |y_{43}^q|^2v^2/2} \quad (\text{doublets}), \end{aligned} \quad (8)$$

with the relations:

$$\begin{aligned} \tan \theta_R^q &= \frac{m_q}{m_Q} \tan \theta_L^q \quad (\text{singlets, triplets}), \\ \tan \theta_L^q &= \frac{m_q}{m_Q} \tan \theta_R^q \quad (\text{doublets}), \end{aligned} \quad (9)$$

with $(q, m_q, m_Q) = (u, m_t, m_T)$ and (d, m_b, m_B) , so one of the mixing angles is always dominant, especially in the down-type quark sector. In addition, for the triplets, the relations between

²As pointed out in the introduction, this bare mass term is not related to the Higgs mechanism. It is gauge-invariant and can appear as such in the Lagrangian, or it can be generated by a Yukawa coupling to a scalar multiplet that acquires a VEV $v' \gg v$.

³We write the triplets in the spherical basis, hence, the $\sqrt{2}$ factors stem from the relation between the Cartesian and spherical coordinates of an irreducible tensor operator of rank 1 (vector).

the off-diagonal Yukawa couplings lead to relations between the mixing angles in the up-and down-type quark sectors,

$$\begin{aligned}\sin 2\theta_L^d &= \sqrt{2} \frac{m_T^2 - m_t^2}{m_B^2 - m_b^2} \sin 2\theta_L^u & (XTB), \\ \sin 2\theta_L^d &= \frac{1}{\sqrt{2}} \frac{m_T^2 - m_t^2}{m_B^2 - m_b^2} \sin 2\theta_L^u & (TBY).\end{aligned}\tag{10}$$

The masses of the heavy VLQs deviate from M^0 due to the non-zero mixing with the SM quarks and for doublets and triplets, the masses of the different components of the multiplet are related. Altogether, these relations show that all multiplets except the (TB) doublet can be parametrized by a mixing angle, a heavy quark mass and a CP-violating phase that enters some couplings, with the latter being ignored for the observables considered in this paper. In the case of the (TB) doublet, there are two independent mixing angles and two CP-violating phases for the up-and-down-type quark sectors, with - again - the latter set to zero in our analysis. Hereafter, we refer to such a construct as the 2HDM+VLQ scenario, each distinguishing between the singlet, doublet, and triplet cases. In the present paper, though, given the emphasis on T VLQs, as opposed to B VLQs, we will treat the (T) singlet, (XT) and (TB) doublets as well as (XTB) and (TBY) triplets whereas we will not deal with the (B) singlet and (BY) doublet representations, as their study is deferred to a future publication. Finally, as discussed in the abstract, we are bound to work in the so-called ‘‘alignment limit’’ of the 2HDM, wherein we fix $m_h = 125$ GeV (so that the lightest neutral Higgs state of the 2HDM is the discovered one) and we have further taken $m_{12}^2 = m_A^2 \frac{\tan^2 \beta}{1 + \tan^2 \beta}$.

2.2 Implementation and validation

In this subsection, we briefly describe our implementation of the aforementioned BSM model. We have used 2HDMC-1.8.0 [25] as a base platform for our 2HDM+VLQ setup⁴. As a first step, the above Lagrangian components were implemented into FeynRules-2.3 [26] to generate the proper spectrum of masses and couplings. With the help of this program, we have then generated FeynArts-3.11 [27, 28] and FormCalc-9.10 [29, 30] model files as well as Universal FeynRules Output (UFO) interfaces to be used in MadGraph-3.4.2 [31]. As consistency checks, we have verified the cancellation of Ultra-Violet (UV) divergences as well as the renormalization scale independence of some loop-level processes such as $h, H, A \rightarrow \gamma\gamma, \gamma Z$ and gg . Theoretical and experimental constraints are accessible easily from within 2HDMC (perturbativity, vacuum stability, triviality, unitarity, alongside EWPOs) as well as through an interface to both HiggsSignals-3 [32–39] (measurements of the SM-like Higgs state h properties), HiggsBounds-6 [32–39] (null searches for the additional Higgs states H, A and H^\pm). (The latest versions of these tools are now incorporated into HiggsTools [40].) Additionally, SuperIso-v4.1 [41] is utilized for flavour constraints.

2.3 EWPO constraints

EWPOs can restrict severely the parameter space of BSM physics scenarios. In our 2HDM+VLQ setup, for both S and T , we have two additive contributions: one from VLQs and the other

⁴A public release of it is in progress: herein, the analytical expressions for the Feynman rules of the interaction vertices of our 2HDM+VLQ model have been implemented as a new class while several new tree-level VLQ decays have explicitly been coded alongside those of Higgs bosons into VLQs themselves.

from 2HDM Higgses. The latter is very well known, and we have taken it from [15] while the former can be calculated using the approach of Ref. [16], as it has been done in Ref. [17]. However, the approach of Ref. [16] works only for singlet and doublet representation of the new fermions, and cannot be applied to the triplet cases. For all various VLQs models considered here, we have computed the S and T parameters with the use of the aforementioned `FeynArts` and `FormCalc` packages using dimensional regularization. The analytic results were obtained as a combination of standard Passarino-Veltman functions. We checked both analytically and numerically that our results for S and T are UV finite and renormalization scale independent. (Such analytic results for the S and T parameters will be presented in [42].) For the T parameter, we have compared our results to Refs. [16, 17] and found good agreement in the case of singlet and doublet. In the case of the triplet representations (XTB) and (TBY), our result disagrees with Ref. [17]. Furthermore, for the S parameter, our results disagree with those of Ref. [17]. In fact, Ref. [17] simply extends the result of the singlet and doublet cases from Ref. [16] to the triplet one. The author of Ref. [43] derives the correct expression for S and T in the case of the (XTB) triplet using the approach of Ref. [16]. We re-computed from scratch the results for the (XTB) and (TBY) triplet cases, then re-derived S and T in terms of Passarino-Veltman functions and, crucially, did not neglect the external momentum of the gauge bosons. We are confident of the correctness of our findings, as they were derived in two different ways. A major source of disagreement would be the fact that Ref. [17] uses a simple approximation for the S parameter, which consists in neglecting the external momentum of the gauge bosons. We also cross-checked with a new calculation [43, 44] and found good agreement for the T parameter. However, we should mention that, for the S parameter, we use the complete analytical result and, again, did not neglect any external momentum as it is usually the case [44].

2.4 Direct search constraints

While experimental limits on the properties (masses and couplings) of the additional Higgs states of the 2HDM+VLQ can seamlessly be taken into account using the described toolbox, those on VLQs require a separate treatment. Specifically, our study reveals that the oblique parameters S and T impose stringent limits on the VLQ mixing angles. As detailed in [45], this constraint ensures the presence of small mixing angles, thereby consistently avoiding exclusion from the existing LHC limits on VLQ masses and allowing for a broad mass range, starting from 600, GeV as depicted Fig. 1. While this result has been obtained for the singlet case, we have checked that a similar pattern emerges in the case of the doublet and triplet as well.

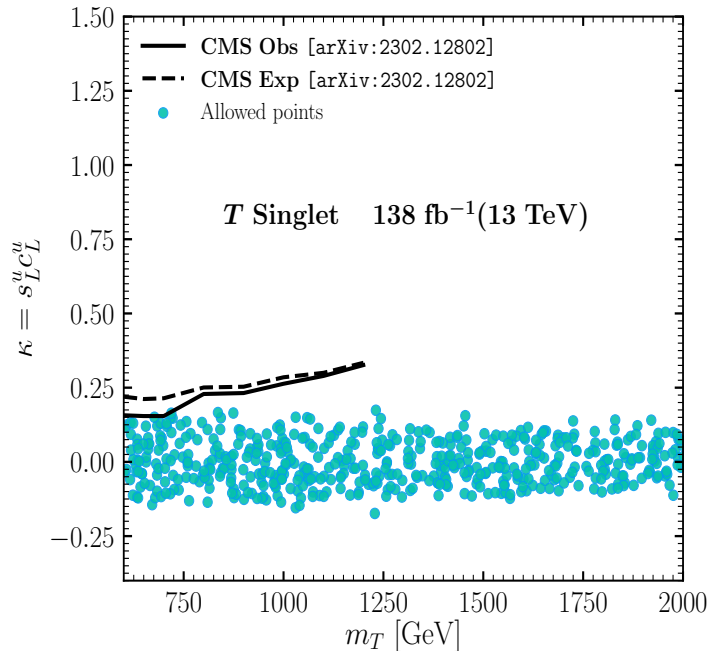


Figure 1: Allowed points following the discussed theoretical and experimental constraints, in the (m_T, κ) plane for the 2HDM+ T singlet scenario, superimposed onto the CMS [46] 95% C.L. observed (solid line) and expected (dashed) upper limits on the coupling κ .

Here, we provide an illustrative example for the singlet case 2HDM+ T , depicting the consistency of our findings against the LHC limits. The blue points representing our results that satisfy all the discussed constraints in the (m_T, κ) plane are overlaid on the 95% Confidence Level (CL) observed (solid) and expected (dashed) contours from CMS [46]. Recalling our earlier discussion on the constraint imposed by the oblique parameters S and T in constraining the VLQ mixing angles to small values, it becomes evident from the figure that our results consistently reside below the observed 95% CL exclusion limit.

3 Results and discussions

3.1 2HDM with (T) singlet

Parameters	Scanned ranges
m_h	125
m_A	[300, 800]
m_H	[300, 800]
m_{H^\pm}	[600, 800]
$\tan \beta$	[1, 20]
m_T	[600, 2000]
$\sin \theta_L^{u,d}$	[-0.5, 0.5]
$\sin \theta_R^{u,d}$	[-0.5, 0.5]

Table 1: 2HDM and VLQs parameters for all scenarios with their scanned ranges. Masses are in GeV. Phases ϕ_u and ϕ_d are set to zero.

In Fig. 2 we perform a scan over the 2HDM parameters (the Higgs masses, $\tan\beta$, $\sin(\beta - \alpha)$, m_{12}) plus the singlet top mass m_T and the (fermionic) mixing angle $\sin\theta_L$, as indicated in Tab. 1. In Fig. 2 (left), we illustrate the results in terms of the contribution of the 2HDM scalars as well as of the only VLQ of this 2HDM+VLQ scenario to the S and T parameters. We do so by showing the two contributions separately as well as summed together. The individual $S_{\text{VLQ}, 2\text{HDM}}$ terms are rather small while the $T_{\text{VLQ}, 2\text{HDM}}$ ones can be large and with opposite sign, thus allowing for strong cancellations, in particular, $T_{2\text{HDM}}$ can have both signs while T_{VLQ} is (nearly) always positive. A large and positive T_{VLQ} is possible for large, $\sin\theta_L$ while a large and negative $T_{2\text{HDM}}$ is possible in the 2HDM with large splitting among heavy Higgs masses. Note that, in this multiplet case, the EWPO constraints from S and T are stronger than R_b limits [10].

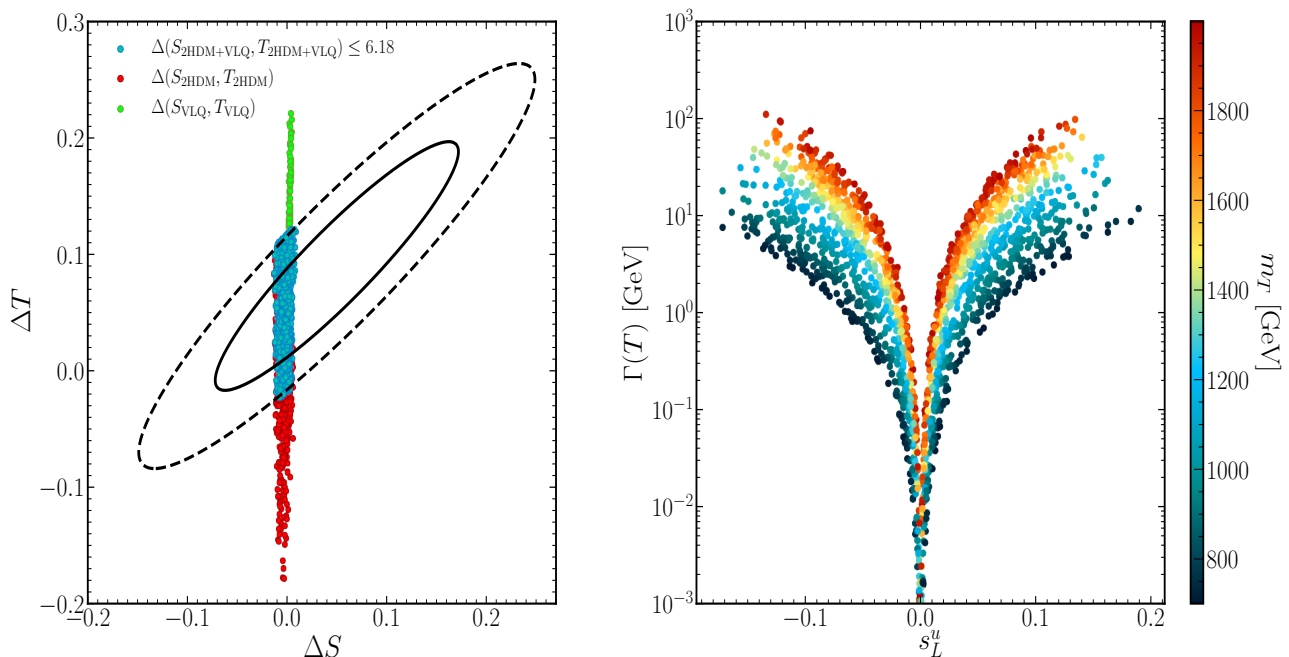


Figure 2: (Left) Scatter plots of randomly generated points superimposed onto the fit limits in the $(\Delta S, \Delta T)$ plane from EWPO data at 95% CL with a correlation of 92%. Here, we illustrate the 2HDM and VLQ contributions separately and also the total one. (Right) The T width $\Gamma(T)(\equiv \Gamma_T)$ as a function of $s_L^u \equiv \sin\theta_L$ with m_T indicated as a colour gauge.

In the right panel of Fig. 2, we project our scan onto the plane $(\sin\theta_L, \Gamma_T)$, where one can see that the mixing angle $|\sin\theta_L|$ is typically constrained to be less than 0.20 for m_T around 700–800 GeV. This value is reduced to approximately 0.05 for $m_T = 2$ TeV. For small mixing, $|\sin\theta_L| < 0.15$, the total width is rather small irrespectively of m_T , of the order few GeV or (much) less, while for large mixing, $|\sin\theta_L| \approx 0.05 - 0.15$, and large m_T , the total width can be in the range 10 – 100 GeV. Hence, it is to be noted that such Γ_T values will probably be comparable with the experimental resolution of reconstructed T states, a regime in which phenomenological implications have been studied in [18, 19] (see also [20–22]). In the end, the T state width can reach at most the 10% level.

Altogether, then, the presence of the additional degrees of freedom of the VLQ sector, combined with those from the 2HDM one, allows for solutions covering rather light m_T values and rather large mixing $|\sin\theta_L|$, to potentially enable significant $pp \rightarrow TT$ production rates at the LHC as well as T decays into heavy (pseudo)scalars Higgs states of 2HDM origin with large probabilities.

We now move on to discuss each Branching Ratio (\mathcal{BR}) of the T state. In the SM with an additional singlet top, the picture is rather simple. The \mathcal{BR} 's of $T \rightarrow W^+b$, $T \rightarrow Zt$ and $T \rightarrow ht$ are approximately around 50%, 25% and 25%, respectively. These three \mathcal{BR} 's are not very sensitive to the mixing angle $\sin \theta_L$ and, further, are not independent of one another, as they satisfy the following sum rule:

$$\mathcal{BR}(T \rightarrow \text{SM}) = \mathcal{BR}(T \rightarrow W^+b) + \mathcal{BR}(T \rightarrow Zt) + \mathcal{BR}(T \rightarrow ht) = 1. \quad (11)$$

(Here, we neglect the decays that are either Cabibbo-Kobayashi-Maskawa (CKM) suppressed or that are loop-mediated, such as $T \rightarrow cg$, $T \rightarrow c\gamma$, etc.) When we add extra (pseudo)scalars, the picture changes drastically because of the presence of new decay channels, such as $T \rightarrow H^+b$, $T \rightarrow At$ and $T \rightarrow Ht$, that could significantly modify the limits coming from T direct searches at the LHC (as explained). The above sum rule will be modified as follows:

$$\begin{aligned} \mathcal{BR}(T \rightarrow \text{SM}) + \mathcal{BR}(T \rightarrow \text{non SM}) &= 1, \\ \mathcal{BR}(T \rightarrow \text{non SM}) &= \mathcal{BR}(T \rightarrow H^+b) + \mathcal{BR}(T \rightarrow At) + \mathcal{BR}(T \rightarrow Ht). \end{aligned} \quad (12)$$

In Fig. 3, we illustrate the correlation between the decays of the T state into SM particles and those via the new channels, paired as follows: $T \rightarrow \{ht, Ht\}$ (left), $T \rightarrow \{Zt, At\}$ (middle) and $T \rightarrow \{W^+b, H^+b\}$ (right). We note that, once the non-SM decays are kinematically open, $\mathcal{BR}(T \rightarrow H^+b)$ would compete with $\mathcal{BR}(T \rightarrow W^+b)$. This is also true for $\mathcal{BR}(T \rightarrow Ht)$ and $\mathcal{BR}(T \rightarrow At)$.

In understanding the numerical results, it is useful to look at the analytical formulae of the Higgs couplings to SM quarks and VLQs (specific to the singlet case), which, in the exact alignment limit, take the following form (in Type-II):

$$\begin{aligned} hTt &= \frac{g}{2M_W} h\bar{t}(\cot \beta m_t c_{LSL} P_L + m_T c_{LSL} P_R)T, \\ HTt &= \frac{g}{2M_W} H\bar{t}(\cot \beta m_t c_{LSL} P_L + \cot \beta m_T c_{LSL} P_R)T, \\ ATt &= \frac{g}{2M_W} A\bar{t}(\cot \beta m_t c_{LSL} P_L + \cot \beta m_T c_{LSL} P_R)T, \\ H^+Tb &= -\frac{gm_T}{\sqrt{2}M_W} H^+\bar{T}(\cot \beta s_L P_L + \frac{m_b}{m_T} \tan \beta s_L)b. \end{aligned}$$

By comparing these formulae to the corresponding ones in the Appendix (Tabs. XVIII–XX, where the full dependence on α and β is retained), we start by noting that, in the alignment limit $\cos(\beta - \alpha) \rightarrow 0$, the $\cot \beta m_t$ term in the hTt coupling comes with a suppression factor $\cos(\beta - \alpha) \approx 0$ while the HTt coupling would come with $\sin(\beta - \alpha) \approx 1$. In contrast, in the case of ATt , there is no $\cos(\beta - \alpha)$ term involved. Further, as one can see from the above couplings, in the case of small $\tan \beta < 2$, the right-handed couplings of HTt and ATt would get more amplification compared to the left-handed ones because of the term $\cot \beta m_T$ and the fact that $m_T \gg m_t$. As for the H^+Tb coupling, which has only a left-handed component, this will also enjoy some enhancement for small $\tan \beta < 2$.

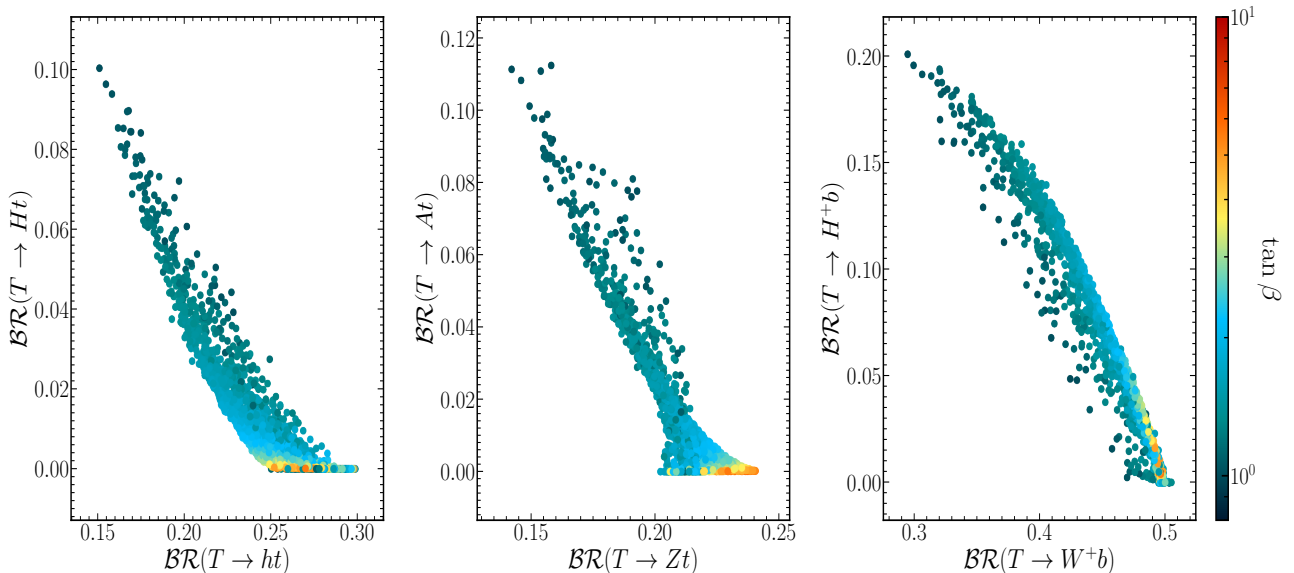


Figure 3: The correlation between $\mathcal{BR}(T \rightarrow ht)$ and $\mathcal{BR}(T \rightarrow Ht)$ (left), $\mathcal{BR}(T \rightarrow Zt)$ and $\mathcal{BR}(T \rightarrow At)$ (middle) as well as $\mathcal{BR}(T \rightarrow W^+b)$ and $\mathcal{BR}(T \rightarrow H^+b)$ (right) with $\tan\beta$ indicated in the colour gauge.

In the light of this, by looking at Fig. 3 (left panel), it is clear why, for small $\tan\beta$, the new channel $T \rightarrow H^+b$ can be sizeable or even dominate $T \rightarrow W^+b$. In contrast, at large $\tan\beta$, we have the opposite situation, $\mathcal{BR}(T \rightarrow H^+b)$ is quite small while $\mathcal{BR}(T \rightarrow W^+b)$ gets close to its SM value. Both effects are due to the singlet heavy top coupling to charged Higgs and bottom quark states, which contains a term $\propto m_T/\tan\beta$. We further stress that, for $\tan\beta \approx 1$, the branching ratios \mathcal{BR} for the exotic decays $T \rightarrow H^+b$, $T \rightarrow At$, and $T \rightarrow Ht$ could reach their maximum values of approximately 20%, 12%, and 10% respectively.

In Fig. 4, we illustrate the T state cumulative \mathcal{BR} 's into SM particles (left panel) and non-SM particles (right panel) as a function of m_T and $\tan\beta$. In both cases, the decay of the heavy singlet top partner is not very sensitive to the first parameter. Further, for small $\tan\beta$, the decays into non-SM particles get amplified as m_T grows and reaches a maximum value of 20%. Conversely, for large $\tan\beta$, irrespectively of m_T , it is the opposite, i.e., the decay into SM particles can become fully dominant.

Thus, having this picture in mind, we initially propose three Benchmark Points (BPs) which are suitable to explore the Type-II scenario of the 2HDM in the presence of a singlet VLQ with top Electromagnetic (EM) charge, as follows.

- i) BP₁: where $\mathcal{BR}(T \rightarrow \text{SM})$ is similar to $\mathcal{BR}(T \rightarrow \text{non SM})$.
- ii) BP₂: where $\mathcal{BR}(T \rightarrow \text{SM})$ is rather small, which makes $\mathcal{BR}(T \rightarrow \text{non SM})$ substantial.
- iii) BP₃: where $\mathcal{BR}(T \rightarrow \text{SM})$ is rather large, which makes $\mathcal{BR}(T \rightarrow \text{non SM})$ marginal.

Input parameters for these BPs are given in Tab. 2.

It should be noted that the presentation of all three BPs depends on the fulfillment of these conditions. In scenarios where not all conditions are met, two BPs may be presented.

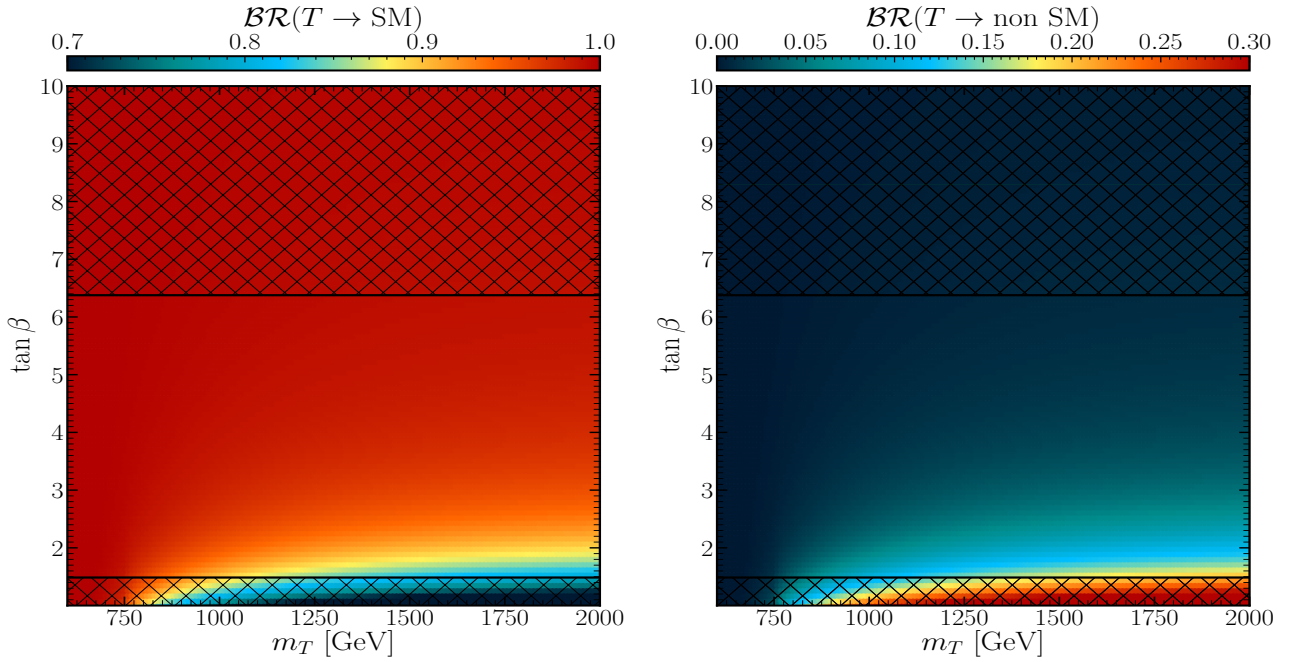


Figure 4: The $\mathcal{BR}(T \rightarrow \text{SM})$ (left) and $\mathcal{BR}(T \rightarrow \text{non SM})$ (right) mapped onto the $(m_T, \tan \beta)$ plane, with $\sin \theta_L = 0.045$, $\sin(\beta - \alpha) = 1$, $m_h = 125$ GeV, $m_H = 585$, $m_A = 582$ GeV, and $m_{H^\pm} = 650$ GeV (recall that $m_{12}^2 = m_A^2 \tan \beta / (1 + \tan^2 \beta)$). Here, the shaded areas are excluded by HiggsBounds ($H^+ \rightarrow t\bar{b}$ [47] for $\tan \beta < 2$ and $H \rightarrow \tau\tau$ [48] for $\tan \beta > 6$). All other constraints (S , T , HiggsSignals, SuperIso and theoretical ones) are also checked.

Parameters	BP ₁	BP ₂
Masses are in GeV		
m_h	125	125
m_H	786.397	713.242
m_A	574.51	654.35
m_{H^\pm}	762.499	767.022
$\tan \beta$	1.004	5.616
m_T	1836.344	1097.177
$\sin(\theta^u)_L$	-0.100	-0.068
$\mathcal{BR}(H^\pm \rightarrow XY)$ in %		
$\mathcal{BR}(H^+ \rightarrow t\bar{b})$	85.44	96.33
$\mathcal{BR}(H^+ \rightarrow \tau\nu)$	0.00	3.38
$\mathcal{BR}(H^+ \rightarrow W^+A)$	14.41	0.05
$\mathcal{BR}(B \rightarrow XY)$ in %		
$\mathcal{BR}(T \rightarrow W^+b)$	29.49	49.65
$\mathcal{BR}(T \rightarrow Zt)$	14.22	22.92
$\mathcal{BR}(T \rightarrow ht)$	15.10	27.00
$\mathcal{BR}(T \rightarrow Ht)$	10.03	0.01
$\mathcal{BR}(T \rightarrow At)$	11.12	0.01
$\mathcal{BR}(T \rightarrow H^-b)$	20.04	0.41
Γ in GeV		
$\Gamma(T)$	68.30	3.98

Table 2: The full description of our BPs for the (T) singlet case.

3.2 2HDM with (TB) doublet

We now discuss the case of the (TB) doublet. In the SM extended with such a VLQ multiplet, both mixing angles in the up- and down-type quark sectors enter the phenomenology of the model⁵. For given θ_R^b , θ_R^t and m_T mass, the relationship between the mass eigenstates and the mixing angles reads as [10]:

$$m_B^2 = (m_T^2 \cos^2 \theta_R^t + m_t^2 \sin^2 \theta_R^t - m_b^2 \sin^2 \theta_R^b) / \cos^2 \theta_R^b, \quad (13)$$

from where one can compute the m_B value. Furthermore, using Eqs. (8)–(9), one can also compute the left mixing θ_L^b and θ_L^t .

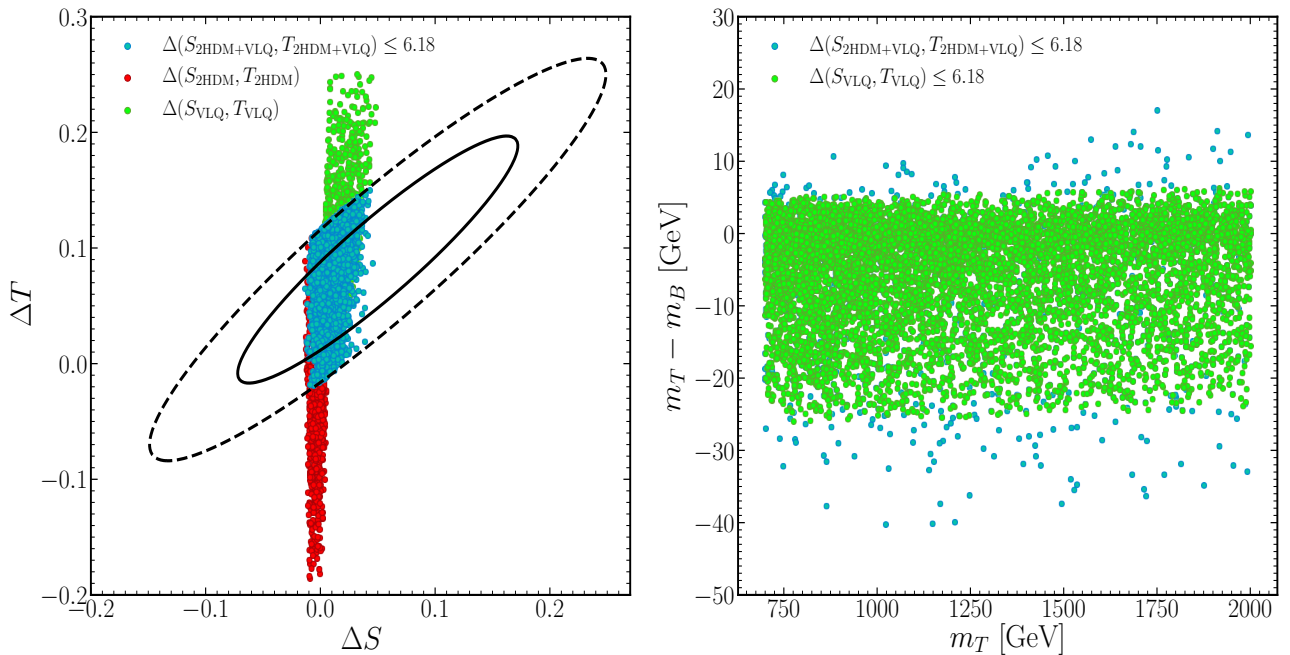


Figure 5: (Left) Scatter plots of randomly generated points superimposed onto the fit limits in the $(\Delta S, \Delta T)$ plane from EWPO data at 95% CL with a correlation of 92%. Here, we illustrate the 2HDM and VLQ contributions separately and also the total one. (Right) The same points are mapped onto the (m_T, δ) plane, where δ is the mass difference between T and B . Here, we only present the VLQ contribution and the total one. Further, all constraints have been taken into account.

In this representation of the 2HDM+VLQ, using the scan ranges in Tab. 1, we illustrate in Fig. 5 the S and T parameters and separate therein the VLQ contribution from the pure 2HDM one. From Fig. 5 (left), like in the previous case of singlet heavy top (T), it is clear that the contribution of the VLQ (TB) doublet and 2HDM states can be of opposite sign, which could then drastically modify the constraints on the parameter space of the model stemming from EWPOs. Further, from Fig. 5 (right), one can see that, for the SM with the VLQ contribution only, the mass splitting between T and B is required to be smaller than 5 GeV in the positive direction and 25 GeV in the negative one while in the case of the 2HDM with VLQs the splitting gets larger by almost a factor of 2. Therefore, we see again that the interplay between the additional VLQ and 2HDM states releases a substantial region of parameter space which would be otherwise unavailable to each BSM setup separately, crucially enabling VLQ

⁵Hereafter, we replace the d and u superscripts in the mixing angles with b and t , respectively.

decays into each other. Specifically, in the case of the SM with a VLQ (TB) doublet, the new top can decay via one of the following modes: $T \rightarrow \{W^+b, Zt, th, BW^+\}$. We remind the reader here that, for vanishing θ_R^t , the couplings tTZ and tTh vanish and T would decay dominantly into W^+b . However, when the mixing does not vanish, the above T decays can proceed simultaneously with \mathcal{BR} 's dependent on the values of the mixing as well as of the VLQ masses. In the presence of extra Higgses, though, one can also have one or more of the following new channels open: $T \rightarrow \{At, Ht, H^+b, H^+B\}$ for T . We are keen to explore their relevance.

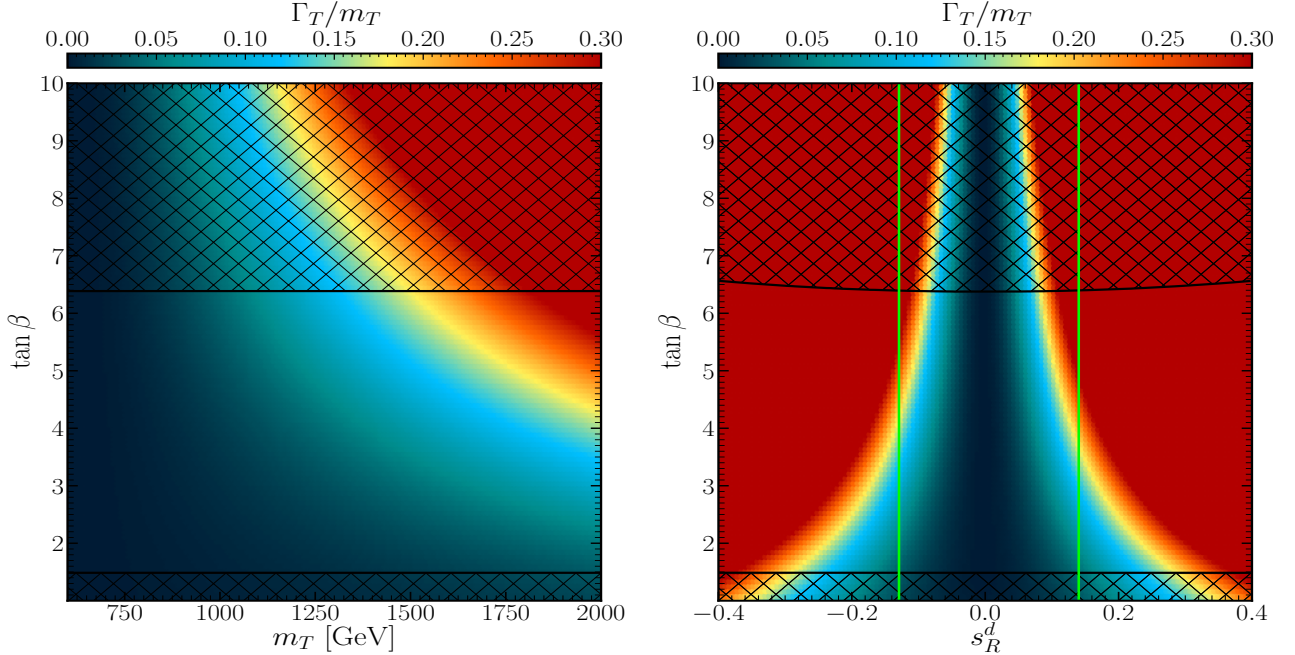


Figure 6: The $\Gamma(T)/m_T$ ratio ($\Gamma(T) \equiv \Gamma_T$) mapped over the $(m_T, \tan\beta)$ plane (left) and $(s_R^d \equiv \sin\theta_R^d, \tan\beta)$ plane (right), with $\sin\theta_R^u = 0.042$ in the left panel and $m_T = 1600$ GeV in the right panel (the 2HDM parameters are the same as in Fig. 4). Here, the shaded areas are excluded by HiggsBounds. The regions between the vertical line green lines are allowed by the S, T parameter constraints, all other constraints (HiggsSignals, SuperIso and theoretical ones) are also checked.

To illustrate the phenomenology of this BSM setup, we exploit again the systematic scan over the 2HDM parameters as well as on the VLQ (TB) doublet ones described in Tab. 1, as usual, in the presence of all theoretical and experimental constraints, as previously discussed. Following such a scan, in Fig. 6, we show the total width of the T state as a function of the T mass (left frame) as well as of the up-quark sector mixing angle (right frame), both correlated to $\tan\beta$. In this setup, we see from the first plot that Γ_T/m_T grows substantially with $\tan\beta$, so as to justify the beyond the Narrow Width Approximation (NWA) of Refs. [18–22], it is worth noting from the second plot that this happens for rather large mixing and small $\tan\beta$ (around 2).

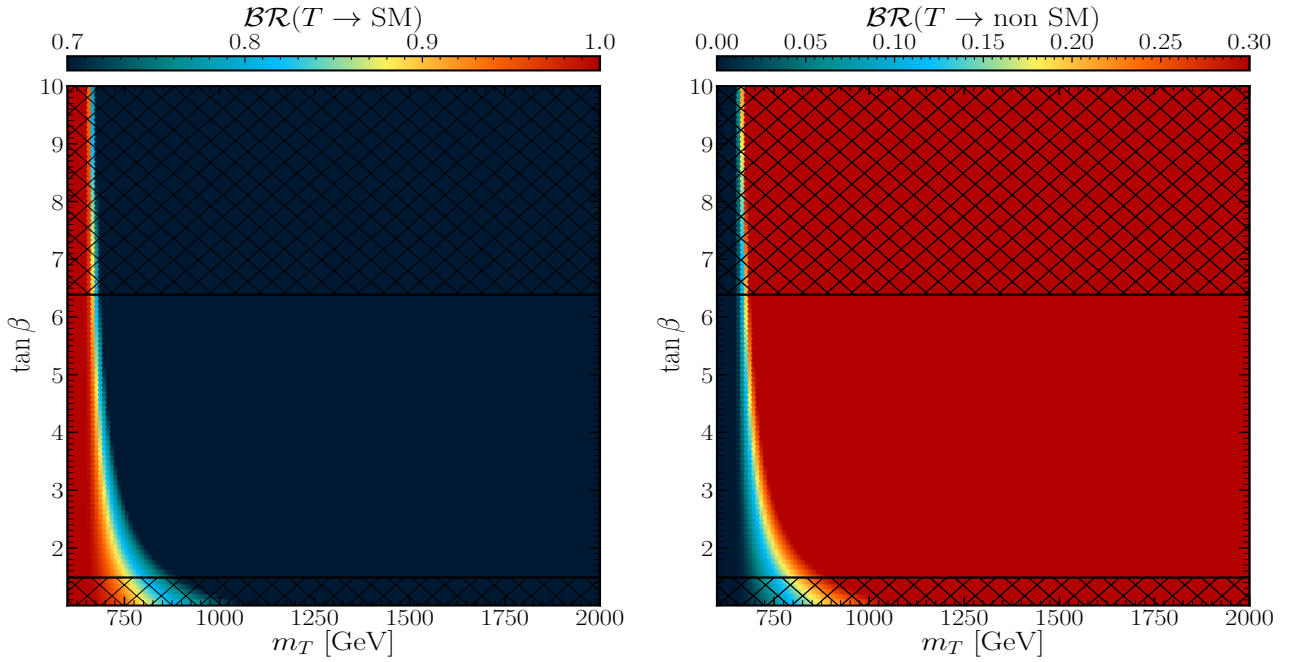


Figure 7: The $\mathcal{BR}(T \rightarrow \text{SM})$ (left) and $\mathcal{BR}(T \rightarrow \text{non SM})$ (right) mapped onto the $(m_T, \tan \beta)$ plane, with the same description as in Fig. 6 (left).

In Fig. 7 we show the correlations between the T decays into SM and non-SM particles, the latter involving one additional Higgs state, such as $T \rightarrow bH^\pm$, $T \rightarrow At$ and $T \rightarrow Ht$ ⁶. One can see from this figure that it is possible to have clear dominance for non-SM T decays over a substantial region of parameter space.

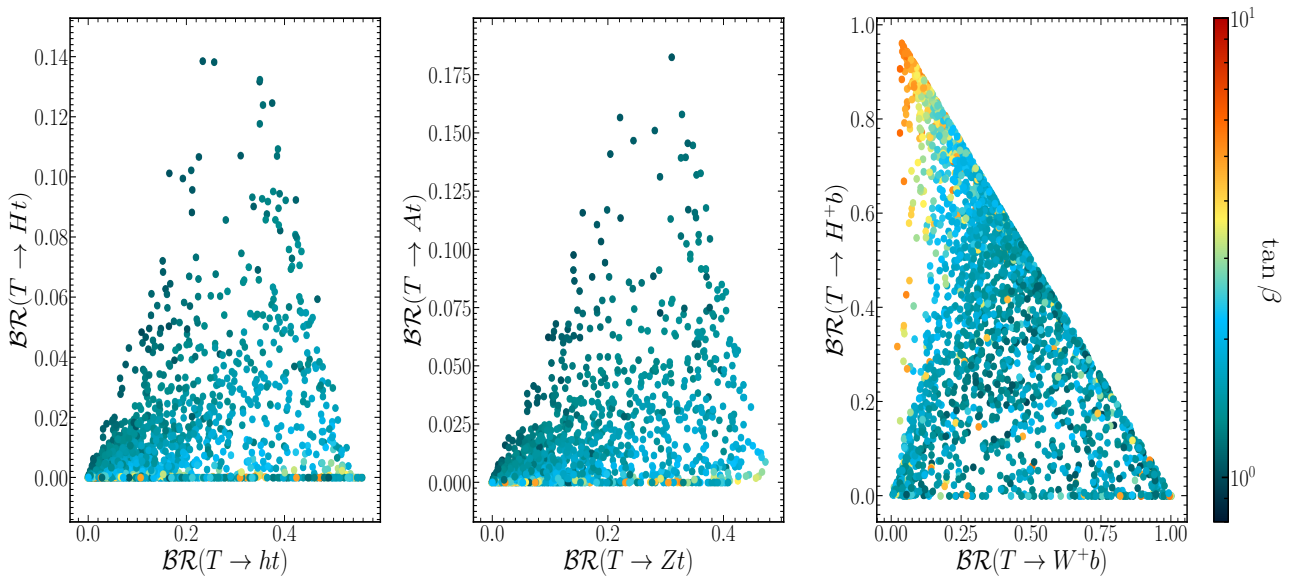


Figure 8: The correlation between $\mathcal{BR}(T \rightarrow ht)$ and $\mathcal{BR}(T \rightarrow Ht)$ (left), $\mathcal{BR}(T \rightarrow Zt)$ and $\mathcal{BR}(T \rightarrow At)$ (middle) as well as $\mathcal{BR}(T \rightarrow W^+b)$ and $\mathcal{BR}(T \rightarrow H^+b)$ (right) with $\tan \beta$ indicated in the colour gauge.

Furthermore, in Fig. 8, we look again at the correlations between the individual SM and

⁶In principle, in the definition of these two \mathcal{BR} 's, one should account for the $T \rightarrow W^+B$ and $T \rightarrow H^+B$ decays, however, because both the W^+ and H^+ are off-shell, they are always small, so we will not discuss these.

non-SM decay channels, using the same pairing as previously. Herein, it is noticeable that, in the neutral current case, the latter is generally smaller than the former while, in the charged current case, $T \rightarrow H^+b$ can dominate $T \rightarrow W^+b$. One can also read that these last two decays are anti-correlated as a function of $\tan \beta$. The dominance of $T \rightarrow W^+b$ corresponds to small, $\tan \beta$ while the dominance of $T \rightarrow H^+b$ prefers medium $\tan \beta$. Like in the case of the SM with a VLQ doublet (TB), also in the case of the 2HDM counterpart, with a vanishing up-type quark mixing, the couplings tTZ and tTA vanish while in $T\bar{H}^-b$ it only remains the term Z_R^{Tb} , which is proportional to m_b and is therefore suppressed at small $\tan \beta$. In the middle(right) panel of Fig. 7, it is clear that the maximum reach for $\mathcal{BR}(T \rightarrow Zt)$ and $\mathcal{BR}(T \rightarrow At)$ ($\mathcal{BR}(T \rightarrow ht)$ and $\mathcal{BR}(T \rightarrow Ht)$) is around 50% and 18%(60% and 14%), respectively. In fact, at large $\tan \beta$, the couplings tTH and tTA are suppressed, being proportional to $\cot \beta$. Therefore, both $T \rightarrow At$ and $T \rightarrow Ht$ are generally suppressed in this limit, which makes $T \rightarrow Zt$ and $T \rightarrow ht$ rather substantial.

Parameters	BP ₁	BP ₂	BP ₃
Masses are in GeV			
m_h	125	125	125
m_H	795.62	596.43	633.50
m_A	651.16	590.06	626.61
m_{H^\pm}	675.46	646.07	673.95
$\tan \beta$	1.60	5.11	3.36
m_T	1322.17	1897.28	1248.85
m_B	1325.44	1898.59	1245.98
$\sin(\theta^u)_L$	0.00785	0.00073	0.00948
$\sin(\theta^d)_L$	0.00033	-0.00010	0.00001
$\sin(\theta^u)_R$	0.06001	0.00807	0.06841
$\sin(\theta^d)_R$	0.09198	-0.03795	0.00167
$\mathcal{BR}(H^\pm \rightarrow XY)$ in %			
$\mathcal{BR}(H^+ \rightarrow tb)$	99.80	95.83	99.21
$\mathcal{BR}(H^+ \rightarrow \tau\nu)$	0.03	3.93	0.59
$\mathcal{BR}(H^+ \rightarrow W^+A)$	0.00	0.00	0.01
$\mathcal{BR}(T \rightarrow XY)$ in %			
$\mathcal{BR}(T \rightarrow W^+b)$	35.20	4.66	1.91
$\mathcal{BR}(T \rightarrow W^+B)$	-	-	-
$\mathcal{BR}(T \rightarrow Zt)$	7.07	0.10	45.52
$\mathcal{BR}(T \rightarrow ht)$	7.92	0.11	51.72
$\mathcal{BR}(T \rightarrow Ht)$	0.51	0.00	0.23
$\mathcal{BR}(T \rightarrow At)$	0.60	0.00	0.19
$\mathcal{BR}(T \rightarrow H^+b)$	48.70	95.13	0.43
$\mathcal{BR}(T \rightarrow H^+B)$	-	-	-
Γ in GeV			
$\Gamma(T)$	18.28	69.35	3.09

Table 3: The full description of our BPs for the (TB) doublet case.

As done in the previous section, we finish this one by presenting again, in Tab. 3, three BPs amenable to experimental investigation, wherein we target T masses (with Γ_T small) just beyond the current experimental limit that we have found (BP₃) alongside two heavier mass

values, in BP_1 and BP_2 , wherein one has a rather narrow and wide T state, respectively, both of which might well be within the reach of the full Run 3 of the LHC.

3.3 2HDM with (XT) doublet

In the case of the SM extended with a (XT) doublet, the ensuing VLQ structure is fully described by the θ_R^t mixing angle and the new top mass m_T . In fact, for a given θ_R^t value, θ_L^t is computed using Eq. (9). The mass of the new VLQ with exotic EM charge $(+5/3)$, the X state, is given as a function of such a mixing angle, m_T , as well as m_t by [10].

$$m_X^2 = m_T^2 \cos^2 \theta_R + m_t^2 \sin^2 \theta_R. \quad (14)$$

This is independent (at tree level) from the additional parameters entering the 2HDM Higgs sector, however, the latter impinges on the viability of this BSM construct against EWPO data.

Following the scan described in Tab. 1, in Fig. 9 (left), we demonstrate that even though the pure contributions of VLQ and 2HDM alone are (largely) out of the allowed EWPO data ellipses, the total contribution VLQ+2HDM falls within the allowed range for ΔS and ΔT . In the right panel of Fig. 9, we further illustrate the size of the mass splitting $\delta = m_T - m_X$ allowed by EWPO data. In the case of the VLQ-only structure, the splitting is always very small. Instead, in the case of the full 2HDM+VLQ scenario, one can see that the splitting could be very large, of the order of 40 GeV, the more so the larger m_T .

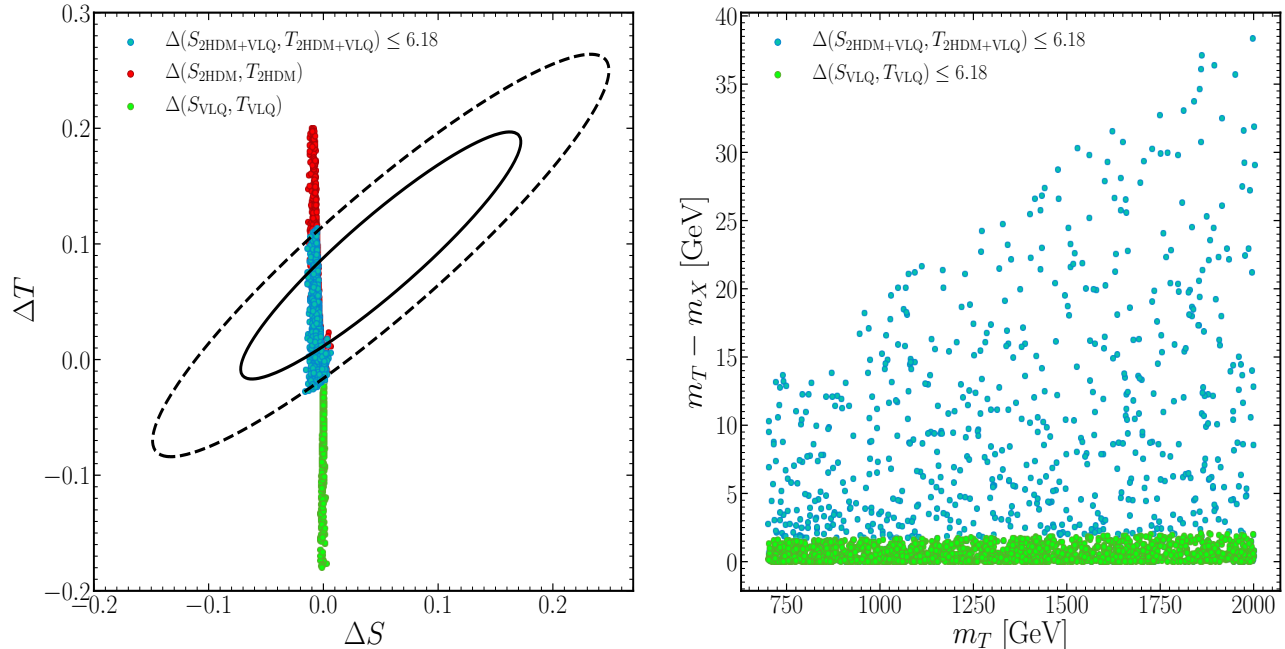


Figure 9: (Left) Scatter plots of randomly generated points superimposed onto the fit limits in the $(\Delta S, \Delta T)$ plane from EWPO data at 95% CL with a correlation of 92%. Here, we illustrate the 2HDM and VLQ contributions separately and also the total one. (Right) The same points are here mapped onto the (m_T, δ) plane, where δ is the mass difference between T and X . Here, we only present the VLQ contribution and the total one. Further, all constraints have been taken into account.

In Fig. 10, we compare again $\mathcal{BR}(T \rightarrow \text{SM})$ to $\mathcal{BR}(T \rightarrow \text{non SM})$, mapped over m_T and $\tan \beta$. In contrast to the previous VLQ doublet realization, here, the latter are sub-leading concerning the former, altogether hardly relevant phenomenological and only very close to the edges of the available parameter space.

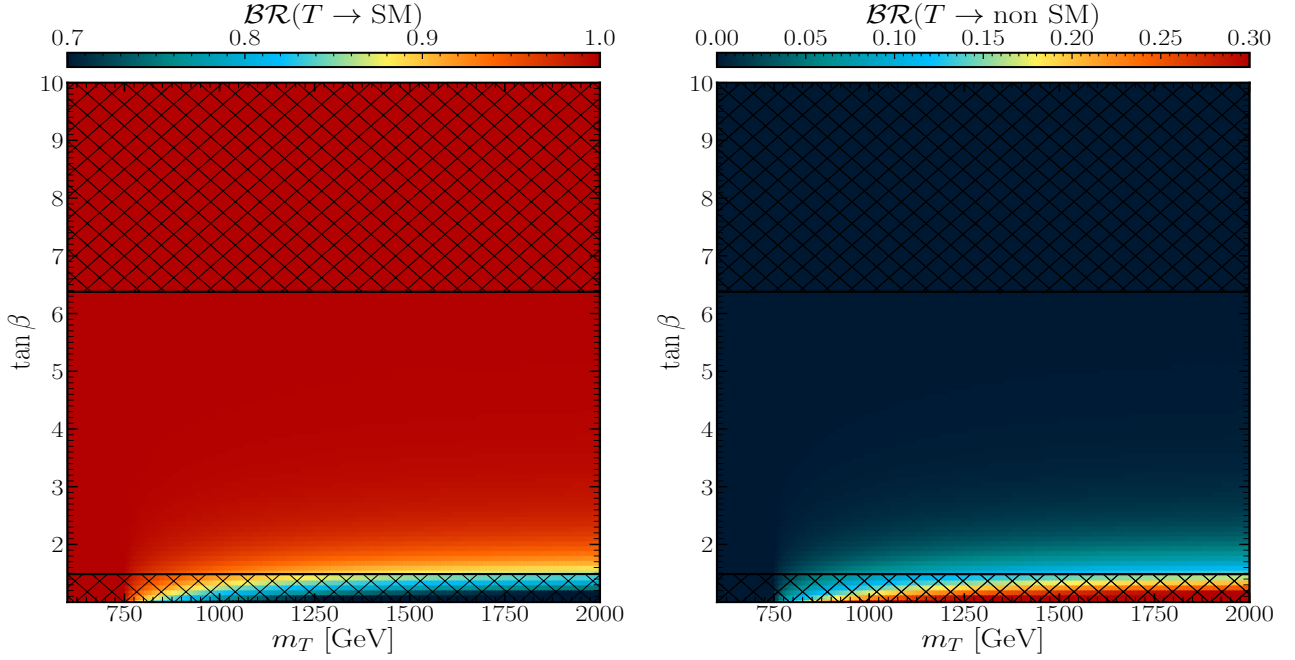


Figure 10: The $\mathcal{BR}(T \rightarrow \text{SM})$ (left) and $\mathcal{BR}(T \rightarrow \text{non SM})$ (right) mapped onto the $(m_T, \tan \beta)$ plane. with $\sin \theta_R^u = 0.057$ (the 2HDM parameters are the same as in Fig. 4). Here, the shaded areas are excluded by HiggsBounds, and all other constraints (S , T , HiggsSignals, SuperIso and theoretical ones) are also checked.

We now discuss the size of the individual \mathcal{BR} 's of T decays. As usual, alongside the SM decays of new top T , into $\{W^+b, Zt, ht\}$, one has the non-SM decays $T \rightarrow Ht$ and $T \rightarrow At$: remarkably, in fact, the $t \rightarrow H^+b$ channel is not available, as the intervening coupling is identically zero. In Fig. 11, we illustrate (from right to left) the usual correlations between $\mathcal{BR}(T \rightarrow W^+b)$ and $\mathcal{BR}(T \rightarrow H^+b)$ ⁷, $\mathcal{BR}(T \rightarrow Zt)$ and $\mathcal{BR}(T \rightarrow At)$ as well as $\mathcal{BR}(T \rightarrow ht)$ and $\mathcal{BR}(T \rightarrow Ht)$. The $\mathcal{BR}(T \rightarrow W^+b)$ is typically SM-like and is of order few percent. At large $\tan \beta$, both $\mathcal{BR}(T \rightarrow Ht)$ and $\mathcal{BR}(T \rightarrow At)$ are suppressed, leading to both $\mathcal{BR}(T \rightarrow Zt)$ and $\mathcal{BR}(T \rightarrow ht)$ reaching their SM values. At small $\tan \beta$, instead, one can see that both $\mathcal{BR}(T \rightarrow Ht)$ and $\mathcal{BR}(T \rightarrow At)$ are somewhat enhanced and therefore $\mathcal{BR}(T \rightarrow Zt)$ and $\mathcal{BR}(T \rightarrow ht)$ are somewhat suppressed, highlighting this region of parameter space as being the most suitable one for exotic T decay searches (albeit limited to neutral decay currents in this BSM framework). However, in line with the previous figure, none of the exotic (neutral) decay channels is ever very large, never passing the 25% or so \mathcal{BR} value.

⁷Despite the latter is identically zero, we have retained it in the plots for graphical convenience.

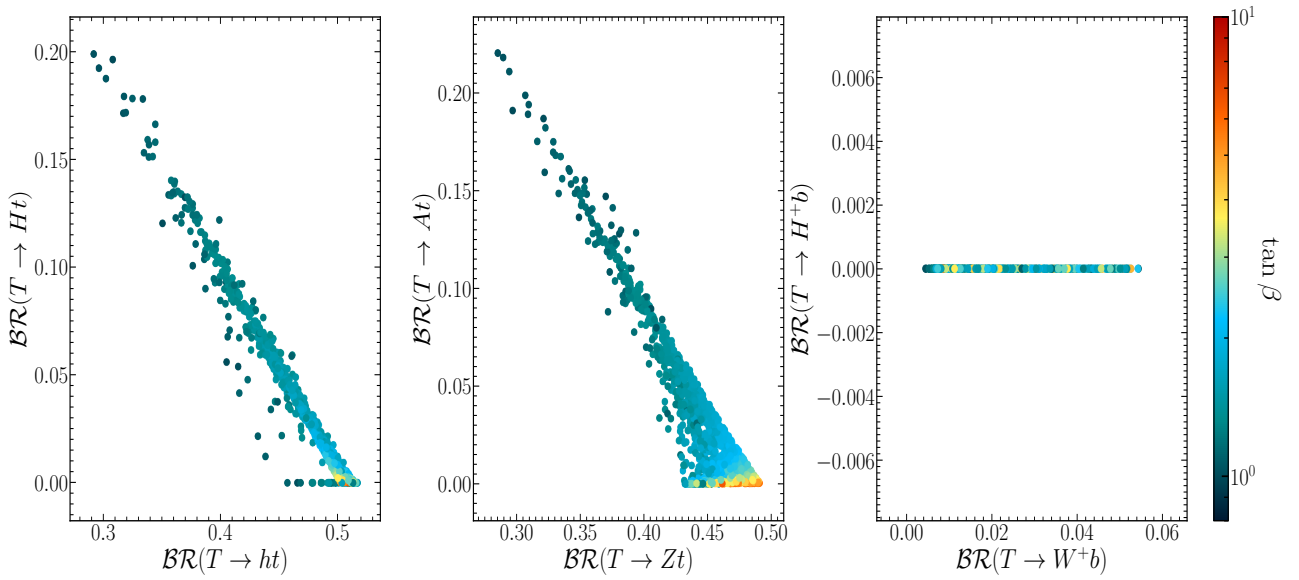


Figure 11: The correlation between $\mathcal{BR}(T \rightarrow ht)$ and $\mathcal{BR}(T \rightarrow Ht)$ (left), $\mathcal{BR}(T \rightarrow Zt)$ and $\mathcal{BR}(T \rightarrow At)$ (middle) as well as $\mathcal{BR}(T \rightarrow W^+b)$ and $\mathcal{BR}(T \rightarrow H^+b)$ with $\tan \beta$ as indicated in the colour gauge.

Parameters	BP ₁	BP ₂
Masses are in GeV		
m_h	125	125
m_H	719.82	561.78
m_A	475.18	550.75
m_{H^\pm}	742.89	685.49
$\tan \beta$	1.03	4.57
m_T	1952.67	1280.43
m_X	1943.95	1264.35
$\sin(\theta^u)_L$	-0.008	-0.022
$\sin(\theta^u)_R$	-0.095	-0.159
$\mathcal{BR}(H^\pm \rightarrow XY)$ in %		
$\mathcal{BR}(H^+ \rightarrow tb)$	56.597	28.527
$\mathcal{BR}(H^+ \rightarrow \tau\nu)$	0.003	0.519
$\mathcal{BR}(H^+ \rightarrow W^+A)$	43.303	42.315
$\mathcal{BR}(T \rightarrow XY)$ in %		
$\mathcal{BR}(T \rightarrow W^+b)$	0.451	1.798
$\mathcal{BR}(T \rightarrow W^+B)$	-	-
$\mathcal{BR}(T \rightarrow Zt)$	28.535	47.801
$\mathcal{BR}(T \rightarrow ht)$	29.184	50.258
$\mathcal{BR}(T \rightarrow Ht)$	19.832	0.077
$\mathcal{BR}(T \rightarrow At)$	21.998	0.066
$\mathcal{BR}(T \rightarrow H^+b)$	-	-
$\mathcal{BR}(T \rightarrow H^+B)$	-	-
Γ in GeV		
$\Gamma(T)$	38.369	18.152

Table 4: The full description of our BPs for the (XT) doublet case.

Finally, the BPs that we recommend for further phenomenological investigation of this BSM scenario are found in Tab. 4, including both a heavy (BP₁) and light (BP₂) T state, the latter being extremely narrow (i.e., the corresponding propagator being essentially a Dirac δ function) in BP₂ and percent level in BP₁ (i.e., probably comparable to the experimental resolution in m_T).

3.4 2HDM with (XTB) triplet

We discuss here the (XTB) triplet case. Before presenting our numerical results, though, let us first introduce our parametrization. This model is fixed by giving the new top mass and one mixing angle, let us say θ_L^t , the other parameters are then computable. In fact, θ_R^t is derived from Eq. (9) while m_X is given by [10]:

$$m_X^2 = m_T^2 \cos^2 \theta_L^u + m_t^2 \sin^2 \theta_L^u = m_B^2 \cos^2 \theta_L^b + m_b^2 \sin^2 \theta_L^b. \quad (15)$$

Using the above relation between m_T and m_X together with the one between up- and down-type quark mixing in Eq. (10), one can derive the mass of the new bottom quark as follows:

$$m_B^2 = \frac{1}{2} \sin^2(2\theta_L^u) (m_T^2 - m_t^2)^2 / (m_X^2 - m_b^2) + m_X^2. \quad (16)$$

The down-type quark mixing is then given by.

$$\sin(2\theta_L^d) = \sqrt{2} \frac{m_T^2 - m_t^2}{m_B^2 - m_b^2} \sin(2\theta_L^u). \quad (17)$$

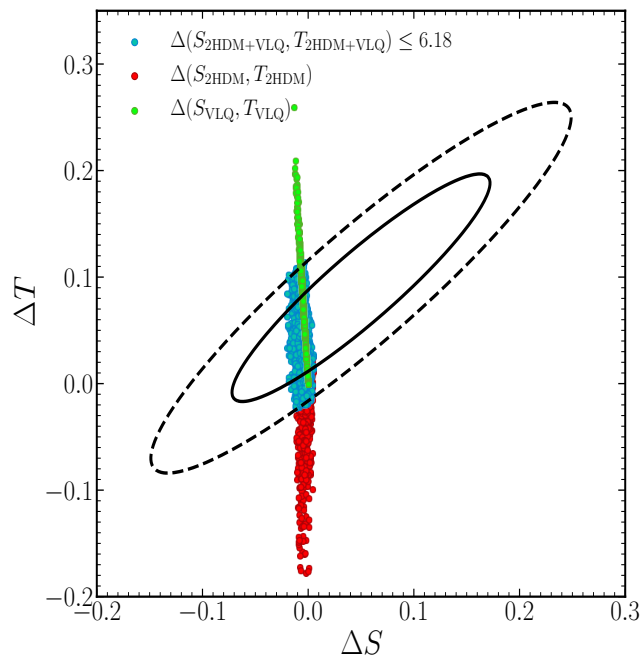


Figure 12: Scatter plots for randomly generated points superimposed onto the fit limits in the $(\Delta S, \Delta T)$ plane from EWPO data at 95% CL with a correlation of 92%. Here, we illustrate the 2HDM and VLQ contributions separately and also the total one. Further, all constraints have been taken into account.

As usual, we perform a systematic scan over both the 2HDM and VLQ parameters, as indicated in Tab. 1. In Fig. 12, we show that, even if 2HDM and VLQ points (mostly) fall out of the allowed ΔS and ΔT ellipses when plotted separately, after adding the 2HDM and VLQ contributions together, one observes that the total contribution can well be within the allowed range.

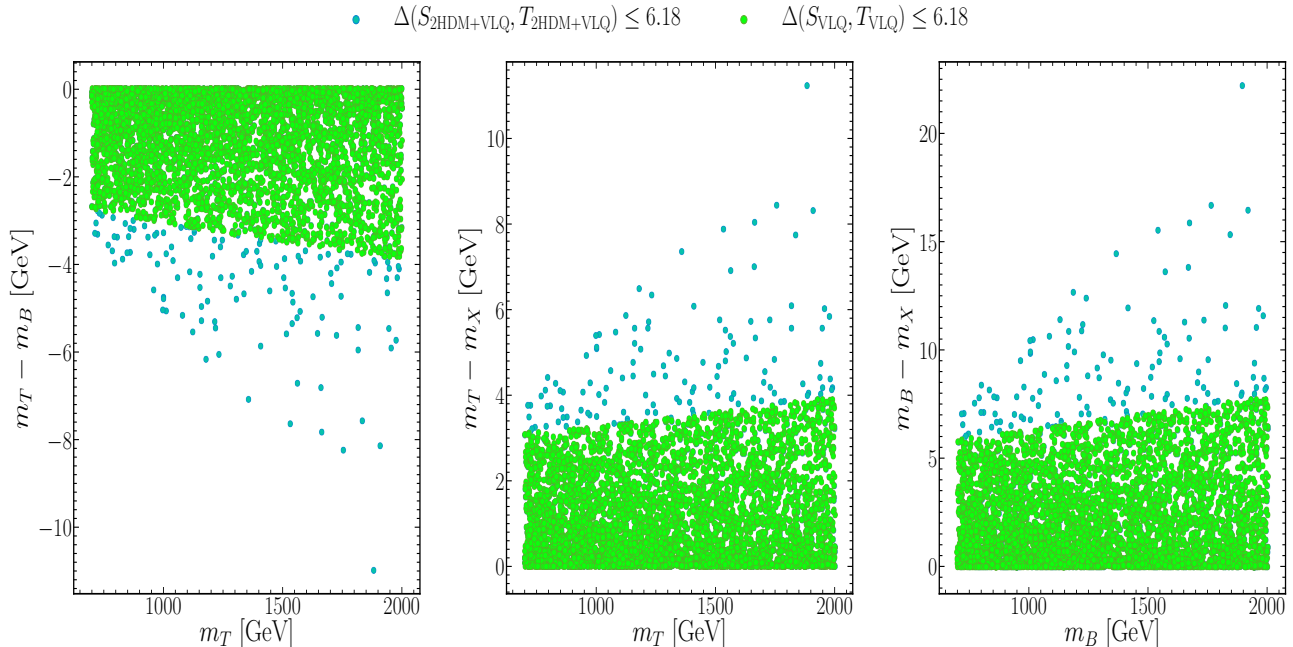


Figure 13: Scatter plots of randomly generated points mapped onto the $(m_{T/B}, \delta)$ plane, where δ is the mass difference between T and B , T and X , and B and X . Here, we illustrate the VLQ and 2HDM+VLQ contributions separately. Further, all constraints have been taken into account.

Furthermore, the splitting between m_T, m_B, m_T, m_X and m_B, m_X is severely constrained by the EWPO constraints (this can be seen in Fig. 13, respectively, mapped against m_T), one can notice that such a splitting is rather small in the case of the SM with VLQ construct, of order a few GeV. However, in the case of the full 2HDM with VLQ scenario, such a splitting becomes large at most 11 or 22 GeV, thereby signalling that inter-VLQ decays are bound to play a negligible role in this BSM realization.

In the case of the 2HDM with a (XTB) triplet, the new top can decay into the following SM channels: $\{Zt, ht, W^+b\}$. Further, it can do so also via the extra channels $\{Ht, At, H^+b\}$, which involves the additional Higgs states of the 2HDM. The relative importance of the former concerning the latter is illustrated in Fig. 14, wherein the dominance of the SM channels is manifest, although the non-SM ones can reach the 20% level in the cumulative \mathcal{BR} 's. We now discuss these individual T decay channels. (Note that, because of the small splitting between X and T , the decay $T \rightarrow W^+X$ is closed for a real W^+ and is very suppressed for an off-shell one, so we do not discuss it here.)

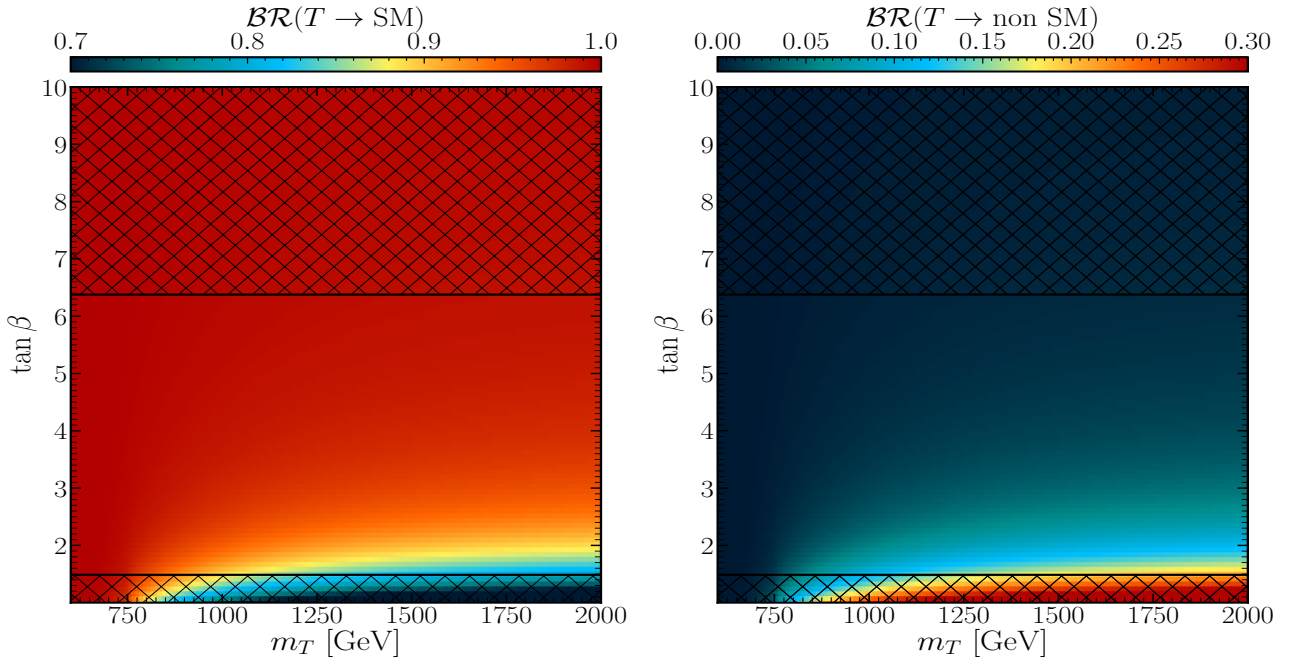


Figure 14: The $\mathcal{BR}(T \rightarrow \text{SM})$ (left) and $\mathcal{BR}(T \rightarrow \text{non SM})$ (right) mapped onto the $(m_T, \tan \beta)$ plane, with $\sin \theta_L^u = 0.0093$ (the 2HDM parameters are the same as in Fig. 4). Here, the shaded areas are excluded by HiggsBounds, and all other constraints (S , T , HiggsSignals, SuperIso and theoretical ones) are also checked.

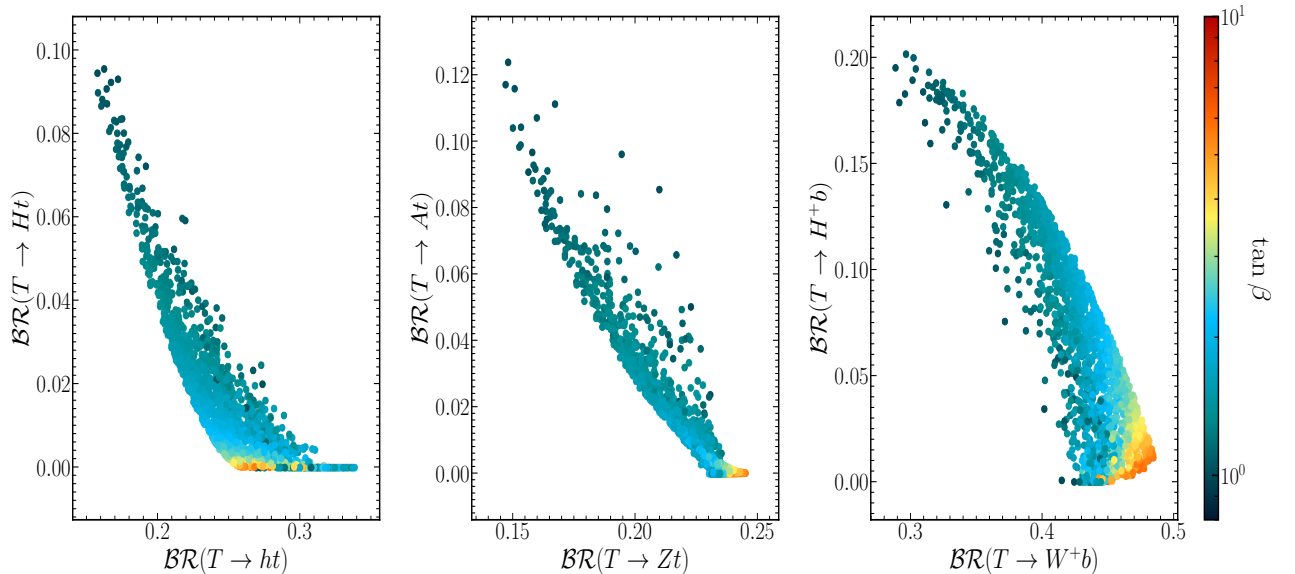


Figure 15: The correlation between $\mathcal{BR}(T \rightarrow ht)$ and $\mathcal{BR}(T \rightarrow Ht)$ (left), $\mathcal{BR}(T \rightarrow Zt)$ and $\mathcal{BR}(T \rightarrow At)$ (middle) as well as $\mathcal{BR}(T \rightarrow W^+b)$ and $\mathcal{BR}(T \rightarrow H^+b)$ (right) with $\tan \beta$ indicated in the colour gauge.

As intimated, the presence of the extra channels, specific to the additional 2HDM states, can change somewhat the SM picture where the new top can decay into one of these final states: $\{Zt, ht, W^+b\}$. In the full 2HDM+VLQ, the new channels $T \rightarrow \{Ht, At, H^+b\}$ could become significant, which implies that simultaneously some SM decays of the new top become suppressed. In fact, we stress that the HTt , ATt and hTt couplings have a term which is proportional to $\cot \beta \sin(\beta - \alpha)$ and this implies that, near the decoupling limit, i.e., $\sin(\beta - \alpha) \approx$

1, those couplings become significant for small $\tan\beta$. Note that the left-handed component of the H^+Tb coupling also has this $\cot\beta$ factor and would enjoy the same enhancement for small $\tan\beta$. These patterns are illustrated in Fig. 15, which however makes it clear that the role of the exotic decays is only relevant at the level of 20% at the most (as expected from the previous figure).

Again, we present our BPs in a table, Tab. 5, two in particular, one with a light T state (BP_2) and one with a heavy T state (BP_1), of varying width, in line with the previous subsections.

Parameters	BP_1	BP_2
Masses are in GeV		
m_h	125	125
m_H	789.60	727.95
m_A	517.79	711.11
m_{H^\pm}	740.65	730.93
$\tan\beta$	1.00	3.11
m_T	1659.95	1109.40
m_B	1666.76	1111.12
m_X	1652.96	1107.58
$\sin(\theta^u)_L$	0.092	0.058
$\sin(\theta^d)_L$	0.128	0.080
$\mathcal{BR}(H^\pm \rightarrow XY)$ in %		
$\mathcal{BR}(H^+ \rightarrow tb)$	69.282	99.403
$\mathcal{BR}(H^+ \rightarrow \tau\nu)$	0.003	0.422
$\mathcal{BR}(H^+ \rightarrow W^+A)$	30.595	0.000
$\mathcal{BR}(T \rightarrow XY)$ in %		
$\mathcal{BR}(T \rightarrow W^+b)$	28.861	46.313
$\mathcal{BR}(T \rightarrow W^+B)$	-	-
$\mathcal{BR}(T \rightarrow Zt)$	14.715	23.836
$\mathcal{BR}(T \rightarrow ht)$	15.837	27.975
$\mathcal{BR}(T \rightarrow Ht)$	9.432	0.097
$\mathcal{BR}(T \rightarrow At)$	11.673	0.077
$\mathcal{BR}(T \rightarrow H^+b)$	19.481	1.702
$\mathcal{BR}(T \rightarrow H^+B)$	-	-
Γ in GeV		
$\Gamma(T)$	41.589	2.918

Table 5: The full description of our BPs for the (XTB) triplet case.

3.5 2HDM with (TBY) triplet

We finally discuss the (TBY) triplet case. In the 2HDM with such a VLQ representation, the situation is very similar to the case of the (T) singlet and (TB) doublet. Before discussing our numerical results, though, let us again first introduce our parametrization. This model is fixed by giving the new top mass and one mixing angle, let us say θ_L^t , the other parameters are then computable. In fact, θ_R^t is derived from Eq. (9) while m_Y is given by [10]:

$$m_Y^2 = m_T^2 \cos^2 \theta_L^t + m_t^2 \sin^2 \theta_L^t = m_B^2 \cos^2 \theta_L^b + m_b^2 \sin^2 \theta_L^b. \quad (18)$$

Using the above relation between m_T and m_Y together with the one between up- and down-type quark mixing in Eq. (10), one can derive the mass of the new bottom quark as:

$$m_B^2 = \frac{1}{8} \sin^2 2\theta_L^t \frac{(m_T^2 - m_t^2)^2}{m_Y^2 - m_b^2} + m_Y^2. \quad (19)$$

With this in hand, one can then derive the down-type quark mixing $\theta_{L,R}^d$ using Eqs. (9)–(10).

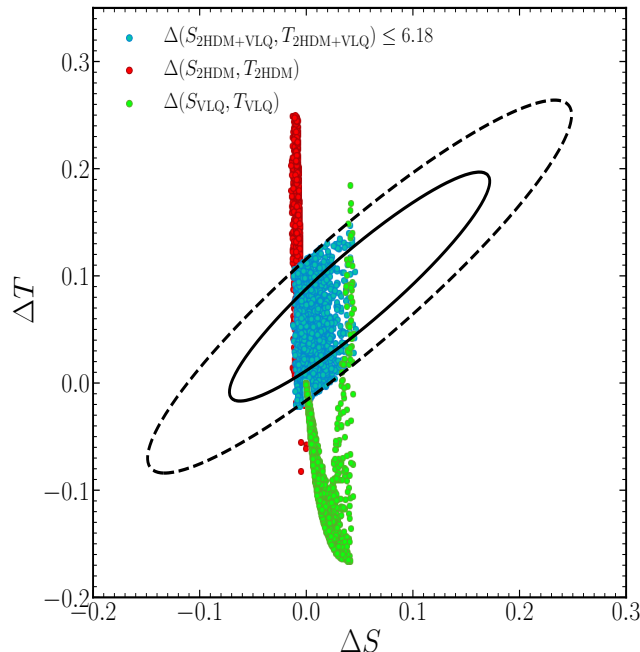


Figure 16: Scatter plots for randomly generated points superimposed onto the fit limits in the $(\Delta S, \Delta T)$ plane from EWPO data at 95% CL with a correlation of 92%. Here, we illustrate the 2HDM and VLQ contributions separately and also the total one. Further, all constraints have been taken into account.

Based on the scan listed in Tab. 1, we first illustrate in Fig. 16 the allowed 95% CL regions from the S and T parameter constraints, which shows that both the 2HDM only and VLQ only contributions could well be out of the allowed ranges but, when adding these together, one indeed finds viable solutions because of cancellations. As mentioned previously, when adding VLQs alongside extra Higgs states, the phenomenology of the S and T can change drastically, with respect to the SM case.

Following Fig. 17, in the SM with this considered VLQ representation, the splitting δ between the masses of T and B (left), T and Y (middle) as well as B and Y (right) is rather small, of the order a fraction of GeV at small m_T . However, for high m_T values, there exists a narrow strip of parameter space where these splittings could be of the order 1 GeV. This is very little. In contrast, in the 2HDM+VLQ case, the situation changes slightly, as the splitting between T and Y could become 3 GeV or more while the ones between T and B as well as B and Y could be up to 5 and 2.5 GeV, respectively. Altogether, yet again, the substantial cancellations between additional Higgs and VLQ states, naturally occurring in loop contributions owing to their different spin statistics, enable one to gain significant parameter space, that we will therefore, in line with the previous two subsections, exploit to study 2HDM decays of VLQ states. Again, though, the small δ values seen in these plots exemplify the fact the VLQ decays into each other are, yet again, mostly negligible.

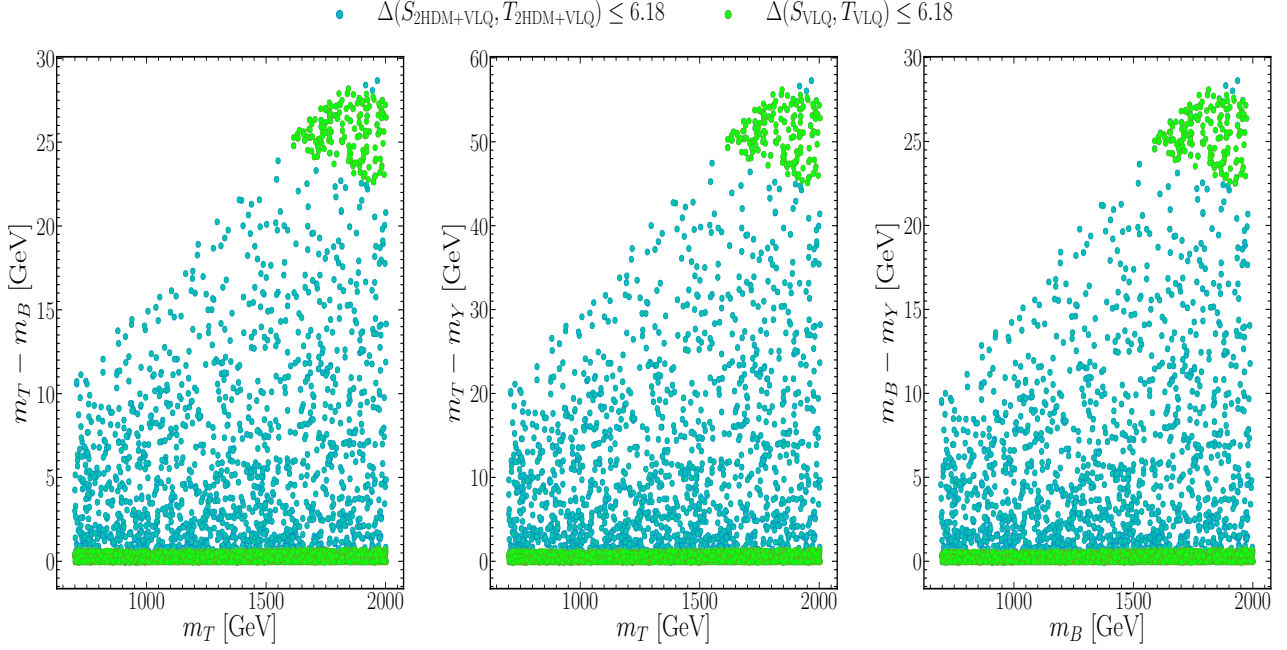


Figure 17: Scatter plots of randomly generated points mapped onto the $(m_{T/B}, \delta)$ plane, where δ is the mass difference between T and B , T and Y , and B and Y . Here, we illustrate the VLQ and 2HDM+VLQ contributions separately. Further, all constraints have been taken into account.

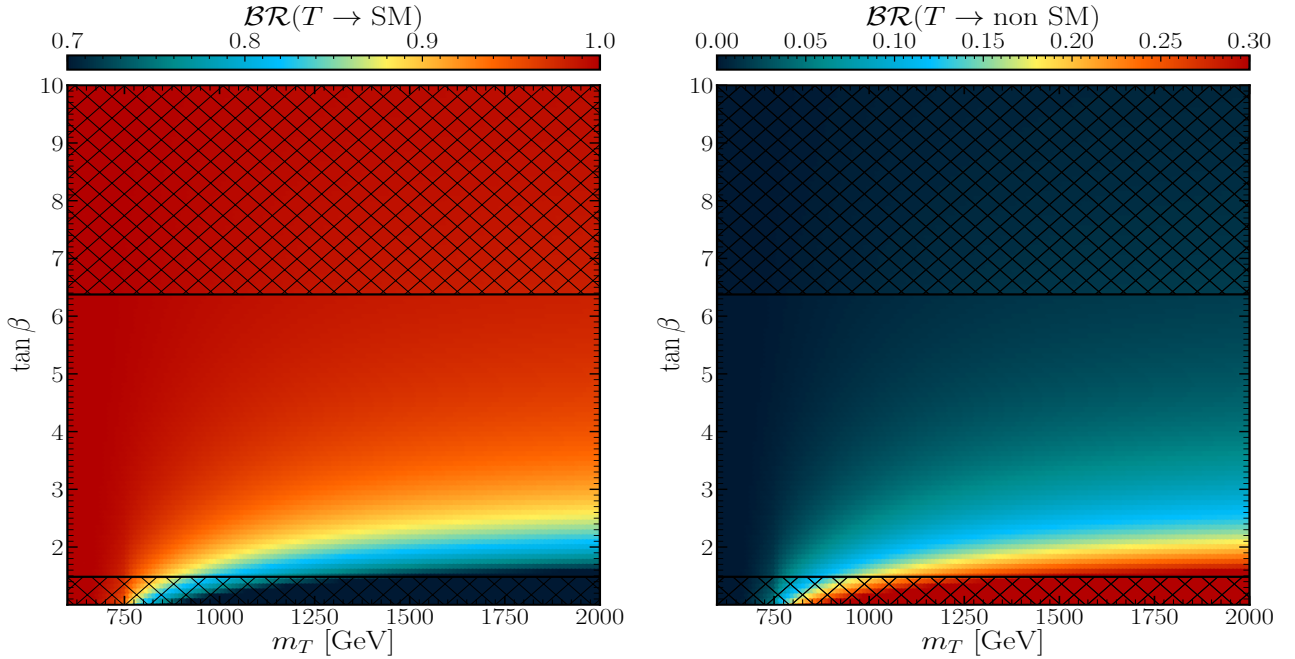


Figure 18: The $\mathcal{BR}(T \rightarrow \text{SM})$ (left) and $\mathcal{BR}(T \rightarrow \text{non SM})$ (right) mapped onto the $(m_T, \tan \beta)$ plane, with $\sin \theta_L^u = 0.02$ (the 2HDM parameters are the same as in Fig. 4). Here, the shaded areas are excluded by HiggsBounds, and all other constraints (S , T , HiggsSignals, SuperIso and theoretical ones) are also checked.

In the SM with a (TBY) triplet, the decay patterns of T states are essentially the same as in the (TB) doublet case, i.e., $T \rightarrow \{W^+b, Zt, ht, W^+B\}$, however, as just intimated, we can neglect the $T \rightarrow W^+B$ case. Therefore, we study in Figs. 18–19, the total SM and non-SM

decays of the T state and the \mathcal{BR} correlations already seen, respectively. In the first figure, we recognize the generally subleading nature of the latter concerning the former. In the second figure, with the \mathcal{BR} 's mapped against $\tan\beta$, it is relevant to notice that the triplet patterns change rather drastically concerning the singlet and doublet ones for the case of T decays, showing a strong anti-correlation between standard and exotic channels, for both charged and (especially) neutral currents. As for the $\tan\beta$ dependence, this is such that large values of it favour the SM decays and small values favour 2HDM ones. Altogether, the exotic channels can have decay rates ranging from about 15% to 30%.

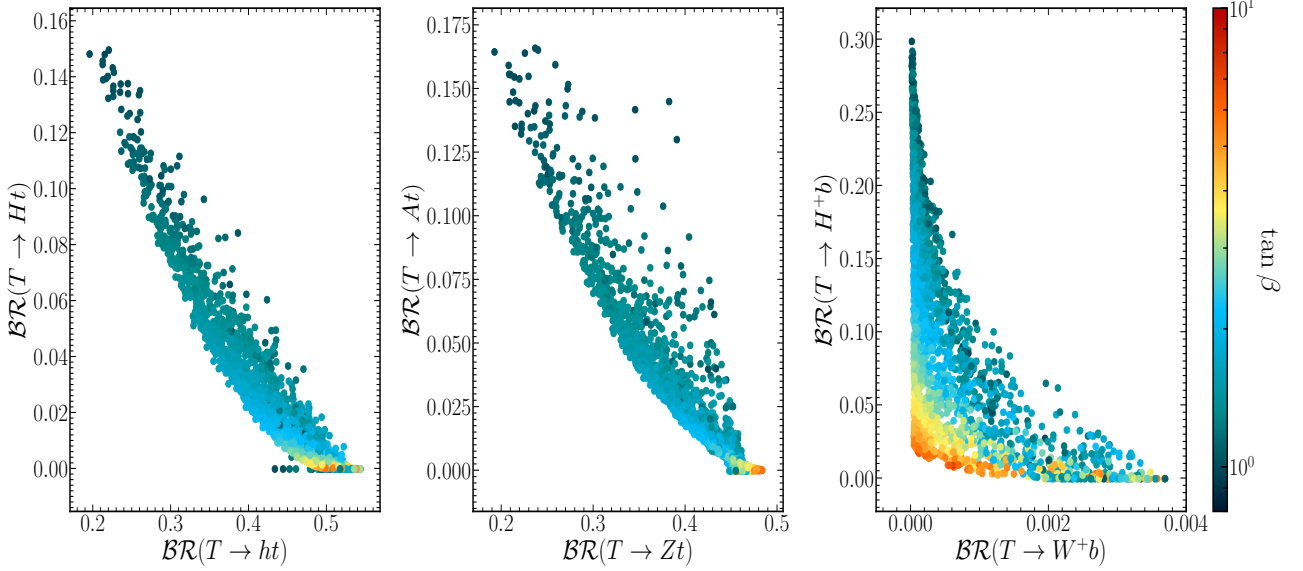


Figure 19: The correlation between $\mathcal{BR}(T \rightarrow ht)$ and $\mathcal{BR}(T \rightarrow Ht)$ (left) (right), $\mathcal{BR}(T \rightarrow Zt)$ and $\mathcal{BR}(T \rightarrow At)$ (middle) as well as $\mathcal{BR}(B \rightarrow W^-t)$ and $\mathcal{BR}(B \rightarrow H^-t)$ (left) with $\tan\beta$ indicated in the colour gauge.

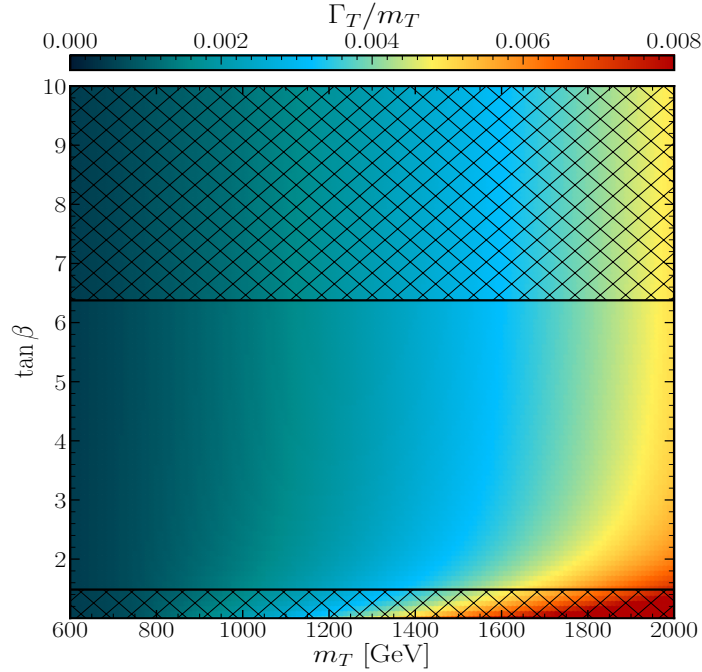


Figure 20: The ratio Γ_T/m_T mapped over the $(m_T, \tan\beta)$ plane. with $\sin\theta_L^u = 0.02$ (the 2HDM parameters are the same as in Fig. 4). Here, the shaded areas are excluded by HiggsBounds, and all other constraints (S , T , HiggsSignals, SuperIso and theoretical ones) are also checked.

Before presenting our BPs, we illustrate in Fig. 20 the ratio Γ_T/m_T , in order to show that, in this BSM scenario, the T state is always very narrow, in fact, the quantity Γ_T/m_T would reach 0.008 at the most and only for high m_T . The BPs themselves are in Tab. 6, wherein the T is always rather heavy, in order to offer some scope to phenomenological studying exotic T decays.

Parameters	BP ₁	BP ₂	BP ₃
Masses are in GeV			
m_h	125	125	125
m_H	744.83	688.06	699.36
m_A	606.08	430.58	690.48
m_{H^\pm}	784.44	696.99	704.26
$\tan\beta$	1.03	1.01	3.55
m_T	1448.05	1916.57	1272.73
m_B	1436.91	1871.83	1271.94
m_Y	1442.41	1894.14	1272.33
$\sin(\theta^u)_L$	0.12	-0.22	-0.04
$\sin(\theta^d)_L$	0.09	-0.15	-0.02
$\mathcal{BR}(H^\pm \rightarrow XY)$ in %			
$\mathcal{BR}(H^+ \rightarrow tb)$	81.41	56.38	99.13
$\mathcal{BR}(H^+ \rightarrow \tau\nu)$	0.00	0.00	0.70
$\mathcal{BR}(H^+ \rightarrow W^+A)$	18.44	43.52	0.00
$\mathcal{BR}(T \rightarrow XY)$ in %			
$\mathcal{BR}(T \rightarrow W^+b)$	0.01	0.00	0.03
$\mathcal{BR}(T \rightarrow W^+B)$	-	-	-
$\mathcal{BR}(T \rightarrow Zt)$	24.80	19.30	46.77
$\mathcal{BR}(T \rightarrow ht)$	25.82	19.70	49.37
$\mathcal{BR}(T \rightarrow Ht)$	12.44	14.77	0.15
$\mathcal{BR}(T \rightarrow At)$	13.69	16.39	0.13
$\mathcal{BR}(T \rightarrow H^+b)$	23.23	29.84	3.53
$\mathcal{BR}(T \rightarrow H^+B)$	-	-	-
Γ in GeV			
$\Gamma(T)$	0.81	0.08	0.85

Table 6: The full description of our BPs for the (TBY) triplet case.

4 Conclusions

The top quark plays a key role in SM dynamics, as it is responsible for the instability of the Higgs mass under radiative corrections, for onsetting the so-called hierarchy problem as well as for the (apparent) metastability of its vacuum. Hence, it is unsurprising that this particle has been heralded as the key messenger of BSM physics. A plausible scenario is that such a state of the SM has one or more companions, i.e., coloured fermionic particles with EM charge $+2/3$, heavier than the top quark itself. However, such new states may not have the same EW properties as the SM object (notably, they cannot be chiral states, i.e., interact with the W^\pm according to a $(1 - \gamma_5)$ current), as this would generate problems about the properties of the discovered Higgs state, both in the SM and in extended Higgs models which possess the SM

limit. An example of the latter is the 2HDM, wherein VLQs can be added to the extended Higgs spectrum, notably, with the same EM charge as the top quark.

Specifically, herein, we have considered a 2HDM of Type-II supplemented by a VLQ companion to the top quark (T), alongside other new fermionic states (B , X and Y), of the SM falling in a singlet, doublet or triplet representation. After constraining the parameter space of this model for all VLQ multiplet cases against theoretical and experimental constraints, we have proceeded to study the ‘standard’ decay $T \rightarrow W^+b, Zt$ and ht (with h the discovered SM-like Higgs state) as well as the ‘exotic’ ones $T \rightarrow H^+b, At$ and Ht (where H^+ , A and H are the heavy Higgs states of the 2HDM). B states were also considered amongst the decay products of the T ones, yet the corresponding channels were typically found negligible.

In doing so, we have shown the following.

- The simultaneous presence of T and additional heavy Higgs boson loops as well as of their mixing effects with t and h states of the SM in the calculation of the EWPOs (i.e., the S, T and U parameters) enables one to access a much wider expanse of parameter space than would otherwise be possible if only the separate effects of, on the one hand, T and, on the other hand, H^+ , A and H states were considered. In particular, this opens up parameter space regions wherein T , as well as H^+ , A and H particles, can be light enough to be pursued in direct searches at the LHC.
- The ability to access the aforementioned T exotic decays (and measure their relative rates when available at the same time) could allow one, in the presence of mass measurements of the Higgs states, to disentangle the underlying VLQ multiplet structure.
- The possibility of accessing all possible exotic decays, in combination with the SM-like ones, could enable one to attempt a fit to the input parameters of our 2HDM plus VLQ model, whichever is its multiplet representation.

We have come to these conclusions by performing an inclusive analysis at the cross-section and \mathcal{BR} level, without any MC simulations. We advocate the latter as the next step to carry out a vigorous research program testing the possibility of both an extended Higgs sector and an enlarged fermionic spectrum being simultaneously accessible at the LHC.

Acknowledgments

We thank R. Enberg, L. Panizzi and S. Taj for their collaboration in the initial stages of this work. The authors have been supported by the grant H2020-MSCA-RISE-2014 no. 645722 (NonMinimalHiggs) in the initial stages of this collaboration. SM is supported in part through the NExT Institute, the STFC Consolidated Grant ST/L000296/1 and the Knut and Alice Wallenberg foundation under the grant KAW 2017.0100 (SHIFT).

Appendix

4.1 Lagrangian in the mass basis

After EWSB, we are left with five Higgs bosons that are two-CP even h and H , one CP-odd A , and then a pair of charged Higgs H^\pm . We now collect the Lagrangian on a mass basis in the general 2HDM.

4.2 Light-light interactions

$$\begin{aligned}
\mathcal{L}_W &= -\frac{g}{\sqrt{2}}\bar{t}\gamma^\mu(V_{tb}^L P_L + V_{tb}^R P_R)bW_\mu^+ + h.c., \\
\mathcal{L}_Z &= -\frac{g}{2c_W}\bar{t}\gamma^\mu(X_{tt}^L P_L + X_{tt}^R P_R - 2Q_t s_W^2)tZ_\mu \\
&\quad -\frac{g}{2c_W}\bar{b}\gamma^\mu(-X_{bb}^L P_L - X_{bb}^R P_R - 2Q_b s_W^2)bZ_\mu + h.c., \\
\mathcal{L}_h &= -\frac{gm_t}{2M_W}Y_{tt}^h\bar{t}t h - \frac{gm_b}{2M_W}Y_{bb}^h\bar{b}b h + h.c., \\
\mathcal{L}_H &= -\frac{gm_t}{2M_W}Y_{tt}^H\bar{t}t H - \frac{gm_b}{2M_W}Y_{bb}^H\bar{b}b H + h.c., \\
\mathcal{L}_A &= -i\frac{gm_t}{2M_W}Y_{tt}^A\bar{t}\gamma_5 t A + i\frac{gm_b}{2M_W}Y_{bb}^A\bar{b}\gamma_5 b A + h.c., \\
\mathcal{L}_{H^\pm} &= -\frac{gm_t}{\sqrt{2}M_W}\bar{t}(\cot\beta Z_{tb}^L P_L + \tan\beta Z_{tb}^R P_R)bH^\pm + h.c.
\end{aligned} \tag{20}$$

	V_{tb}^L	V_{tb}^R
(T)	c_L	$-c_L$
(XT)	c_L	0
(TB)	$c_L^u c_L^d + s_L^u s_L^d e^{i(\phi_u - \phi_d)}$	$s_R^u s_R^d e^{i(\phi_u - \phi_d)}$
(XTB)	$c_L^u c_L^d + \sqrt{2}s_L^u s_L^d$	$\sqrt{2}s_R^u s_R^d$
(TBY)	$c_L^u c_L^d + \sqrt{2}s_L^u s_L^d$	$\sqrt{2}s_R^u s_R^d$

Table VII: Light-light couplings to the W boson.

	X_{tt}^L	X_{tt}^R	X_{bb}^L	X_{bb}^R
(T)	c_L^2	0	1	0
(XT)	$c_L^2 - s_L^2$	$-s_R^2$	1	0
(TB)	1	$(s_R^u)^2$	1	$(s_R^d)^2$
(XTB)	$(c_L^u)^2$	0	$1 + (s_L^d)^2$	$2(s_R^d)^2$
(TBY)	$1 + (s_L^u)^2$	$2(s_R^u)^2$	$(c_L^d)^2$	0

Table VIII: Light-light couplings to the Z boson.

	Y_{tt}^h	Y_{tt}^H	Y_{tt}^A
(T)	$(s_{\beta\alpha} + c_{\beta\alpha} \cot\beta)c_L^2$	$(c_{\beta\alpha} - s_{\beta\alpha} \cot\beta)c_L^2$	$-\cot\beta c_L^2$
(XT)	$(s_{\beta\alpha} + c_{\beta\alpha} \cot\beta)c_R^2$	$(c_{\beta\alpha} - s_{\beta\alpha} \cot\beta)c_R^2$	$-\cot\beta c_R^2$
(TB)	$(s_{\beta\alpha} + c_{\beta\alpha} \cot\beta)(c_R^u)^2$	$(c_{\beta\alpha} - s_{\beta\alpha} \cot\beta)(c_R^u)^2$	$-\cot\beta(c_R^u)^2$
(XTB)	$(s_{\beta\alpha} + c_{\beta\alpha} \cot\beta)(c_L^u)^2$	$(c_{\beta\alpha} - s_{\beta\alpha} \cot\beta)(c_L^u)^2$	$-\cot\beta(c_L^u)^2$
(TBY)	$(s_{\beta\alpha} + c_{\beta\alpha} \cot\beta)(c_L^u)^2$	$(c_{\beta\alpha} - s_{\beta\alpha} \cot\beta)(c_L^u)^2$	$-\cot\beta(c_L^u)^2$

Table IX: Light-light top quark couplings to the triplets Higgs $\{h, H, A\}$.

	Y_{bb}^h	Y_{bb}^H	Y_{bb}^A
(T)	$s_{\beta\alpha} - c_{\beta\alpha} \tan \beta$	$c_{\beta\alpha} + s_{\beta\alpha} \tan \beta$	$\tan \beta$
(XT)	$s_{\beta\alpha} - c_{\beta\alpha} \tan \beta$	$c_{\beta\alpha} + s_{\beta\alpha} \tan \beta$	$\tan \beta$
(TB)	$(s_{\beta\alpha} - c_{\beta\alpha} \tan \beta)(c_R^d)^2$	$(c_{\beta\alpha} + s_{\beta\alpha} \tan \beta)(c_R^d)^2$	$\tan \beta (c_R^d)^2$
(XTB)	$(s_{\beta\alpha} - c_{\beta\alpha} \tan \beta)(c_L^d)^2$	$(c_{\beta\alpha} + s_{\beta\alpha} \tan \beta)(c_L^d)^2$	$\tan \beta (c_L^d)^2$
(TBY)	$(s_{\beta\alpha} - c_{\beta\alpha} \tan \beta)(c_L^d)^2$	$(c_{\beta\alpha} + s_{\beta\alpha} \tan \beta)(c_L^d)^2$	$\tan \beta (c_L^d)^2$

Table X: Light-light bottom quark couplings to the triplets Higgs $\{h, H, A\}$.

	Z_{tb}^L	Z_{tb}^R
(T)	c_L	$\frac{m_b}{m_t} c_L$
(XT)	c_R	$\frac{m_b}{m_t} c_L$
(TB)	$c_L^d c_L^u + \frac{s_L^d}{s_L^u} (s_L^{u2} - s_R^{u2}) e^{i(\phi_u - \phi_d)}$	$\frac{m_b}{m_t} \left[c_L^u c_L^d + \frac{s_L^u}{s_L^d} (s_L^{d2} - s_R^{d2}) e^{i(\phi_u - \phi_d)} \right]$
(XTB)	c_L^u	$\frac{m_b}{m_t} c_L^d$
(TBY)	c_L^u	$\frac{m_b}{m_t} c_L^d$

Table XI: Light-light couplings to the Higgs charged.

4.3 Heavy-heavy interactions

$$\begin{aligned}
\mathcal{L}_W &= -\frac{g}{\sqrt{2}} \bar{Q} \gamma^\mu (V_{QQ'}^L P_L + V_{QQ'}^R P_R) Q' W_\mu^+ + h.c., \\
\mathcal{L}_Z &= -\frac{g}{2c_W} \bar{Q} \gamma^\mu (\pm X_{QQ}^L P_L \pm X_{QQ}^R P_R - 2Q_Q s_W^2) Q Z_\mu \\
\mathcal{L}_h &= -\frac{gm_Q}{2M_W} Y_{QQ}^h \bar{Q} Q h + h.c., \\
\mathcal{L}_H &= -\frac{gm_Q}{2M_W} Y_{QQ}^H \bar{Q} Q H + h.c., \\
\mathcal{L}_A &= \pm i \frac{gm_Q}{2M_W} Y_{QQ}^A \bar{Q} \gamma_5 Q A + h.c., \\
\mathcal{L}_{H^+} &= -\frac{gm_Q}{\sqrt{2}M_W} \bar{Q} (\cot \beta Z_{QQ}^L P_L + \tan \beta Z_{QQ}^R P_R) Q H^+ + h.c.
\end{aligned} \tag{21}$$

	V_{TB}^L	V_{TB}^R
(TB)	$s_L^u s_L^d e^{-i(\phi_u - \phi_d)} + c_L^u c_L^d$	$c_R^u c_R^d$
(XTB)	$s_L^u s_L^d + \sqrt{2} c_L^u c_L^d$	$\sqrt{2} c_R^u c_R^d$
(TBY)	$s_L^u s_L^d + \sqrt{2} c_L^u c_L^d$	$\sqrt{2} c_R^u c_R^d$

Table XII: Heavy-heavy couplings to the W boson.

	X_{TT}^L	X_{TT}^R
(T)	$(s_L)^2$	0
(XT)	$s_L^2 - c_L^2$	$-c_R^2$
(TB)	1	$(c_R^u)^2$
(XTB)	$(s_L^u)^2$	0
(TBY)	$1 + (c_L^u)^2$	$2(c_R^u)^2$

Table XIII: Heavy-heavy couplings to the Z boson.

	Y_{TT}^h	Y_{TT}^H	Y_{TT}^A
(T)	$(s_{\beta\alpha} + c_{\beta\alpha} \cot \beta) s_L^2$	$(c_{\beta\alpha} - s_{\beta\alpha} \cot \beta) s_L^2$	$-\cot \beta s_L^2$
(XT)	$(s_{\beta\alpha} + c_{\beta\alpha} \cot \beta) s_R^2$	$(c_{\beta\alpha} - s_{\beta\alpha} \cot \beta) s_R^2$	$-\cot \beta s_R^2$
(TB)	$(s_{\beta\alpha} + c_{\beta\alpha} \cot \beta) (s_R^u)^2$	$(c_{\beta\alpha} - s_{\beta\alpha} \cot \beta) (s_R^u)^2$	$-\cot \beta (s_R^u)^2$
(XTB)	$(s_{\beta\alpha} + c_{\beta\alpha} \cot \beta) (s_L^u)^2$	$(c_{\beta\alpha} - s_{\beta\alpha} \cot \beta) (s_L^u)^2$	$-\cot \beta (s_L^u)^2$
(TBY)	$(s_{\beta\alpha} + c_{\beta\alpha} \cot \beta) (s_L^u)^2$	$(c_{\beta\alpha} - s_{\beta\alpha} \cot \beta) (s_L^u)^2$	$-\cot \beta (s_L^u)^2$

 Table XIV: Heavy-heavy Top VLQ couplings to the triplets Higgs $\{h, H, A\}$.

	Z_{TB}^L	Z_{TB}^R
(TB)	$s_L^d s_L^u e^{i(\phi_d - \phi_u)} + \frac{c_L^d}{c_L^u} (s_R^u)^2 - s_L^u$	$\frac{m_B}{m_T} \left[s_L^u s_L^d e^{i(\phi_d - \phi_u)} + \frac{c_L^u}{c_L^d} (s_R^d)^2 - s_L^d \right]$
(XTB)	—	—
(TBY)	—	—

Table XV: Heavy-heavy couplings to the Higgs charged.

4.4 Light-heavy interactions

$$\begin{aligned}
 \mathcal{L}_W &= -\frac{g}{\sqrt{2}} \bar{Q} \gamma^\mu (V_{Qq}^L P_L + V_{Qq}^R P_R) q W_\mu^+ \\
 &\quad -\frac{g}{\sqrt{2}} \bar{q} \gamma^\mu (V_{qQ}^L P_L + V_{qQ}^R P_R) Q W_\mu^+ + h.c. \\
 \mathcal{L}_Z &= -\frac{g}{2c_W} \bar{q} \gamma^\mu (\pm X_{qQ}^L P_L \pm X_{qQ}^R P_R) Q Z_\mu + H.c. \\
 \mathcal{L}_h &= -\frac{gm_T}{2M_W} \bar{t} (Y_{htT}^L P_L + Y_{htT}^R P_R) T h \\
 &\quad -\frac{gm_B}{2M_W} \bar{b} (Y_{hbB}^L P_L + Y_{hbB}^R P_R) B h + H.C. \\
 \mathcal{L}_H &= -\frac{gm_T}{2M_W} \bar{t} (Y_{HtT}^L P_L + Y_{HtT}^R P_R) T H \\
 &\quad -\frac{gm_B}{2M_W} \bar{b} (Y_{HbB}^L P_L + Y_{HbB}^R P_R) B h + H.C. \\
 \mathcal{L}_A &= i \frac{gm_T}{2M_W} \bar{t} (Y_{AtT}^L P_L - Y_{AtT}^R P_R) T A \\
 &\quad -i \frac{gm_B}{2M_W} \bar{b} (Y_{AbB}^L P_L - Y_{AbB}^R P_R) B A + H.C. \\
 \mathcal{L}_{H^+} &= -\frac{gm_T}{\sqrt{2}M_W} \bar{T} (\cot \beta Z_{Tb}^L P_L + \tan \beta Z_{Tb}^R P_R) b H^+ \\
 &\quad -\frac{gm_B}{\sqrt{2}M_W} \bar{t} (\cot \beta Z_{tB}^L P_L + \tan \beta Z_{tB}^R P_R) B H^+ + H.c., \tag{22}
 \end{aligned}$$

	V_{Tb}^L	V_{Tb}^R
(T)	$s_L e^{-i\phi}$	0
(XT)	$s_L e^{-i\phi}$	0
(TB)	$s_L^u c_L^d e^{-i\phi_u} - c_L^u s_L^d e^{-i\phi_d}$	$-c_R^u s_R^d e^{-i\phi_d}$
(XTB)	$(s_L^u c_L^d - \sqrt{2} c_L^u s_L^d) e^{-i\phi}$	$-\sqrt{2} c_R^u s_R^d e^{-i\phi}$
(TBY)	$(s_L^u c_L^d - \sqrt{2} c_L^u s_L^d) e^{-i\phi}$	$-\sqrt{2} c_R^u s_R^d e^{-i\phi}$

Table XVI: Heavy-light couplings to the W boson.

	X_{tT}^L	X_{tT}^R
(T)	$c_L s_L e^{i\phi}$	0
(XT)	$2c_L s_L e^{i\phi}$	$c_R s_R e^{i\phi}$
(TB)	0	$-s_R^u c_R^u e^{i\phi_u}$
(XTB)	$s_L^u c_L^u e^{i\phi}$	0
(TBY)	$-s_L^u c_L^u e^{i\phi}$	$-2s_R^u c_R^u e^{i\phi}$

Table XVII: Light-heavy couplings to the Z boson.

	Y_{htT}^L	Y_{HtT}^L	Y_{AtT}^L
(T)	$(s_{\beta\alpha} + c_{\beta\alpha} \cot \beta) \frac{m_t}{m_T} c_L s_L e^{i\phi}$	$(c_{\beta\alpha} - s_{\beta\alpha} \cot \beta) \frac{m_t}{m_T} c_L s_L e^{i\phi}$	$-\cot \beta \frac{m_t}{m_T} c_L s_L e^{i\phi}$
(XT)	$(s_{\beta\alpha} + c_{\beta\alpha} \cot \beta) c_R s_R e^{i\phi}$	$(c_{\beta\alpha} - s_{\beta\alpha} \cot \beta) c_R s_R e^{i\phi}$	$-\cot \beta c_R s_R e^{i\phi}$
(TB)	$(s_{\beta\alpha} + c_{\beta\alpha} \cot \beta) s_R^u c_R^u e^{i\phi_u}$	$(c_{\beta\alpha} - s_{\beta\alpha} \cot \beta) s_R^u c_R^u e^{i\phi_u}$	$-\cot \beta s_R^u c_R^u e^{i\phi_u}$
(XTB)	$(s_{\beta\alpha} + c_{\beta\alpha} \cot \beta) \frac{m_t}{m_T} s_L^u c_L^u e^{i\phi}$	$(c_{\beta\alpha} - s_{\beta\alpha} \cot \beta) \frac{m_t}{m_T} s_L^u c_L^u e^{i\phi}$	$-\cot \beta \frac{m_t}{m_T} s_L^u c_L^u e^{i\phi}$
(TBY)	$(s_{\beta\alpha} + c_{\beta\alpha} \cot \beta) \frac{m_t}{m_T} s_L^u c_L^u e^{i\phi}$	$(c_{\beta\alpha} - s_{\beta\alpha} \cot \beta) \frac{m_t}{m_T} s_L^u c_L^u e^{i\phi}$	$-\cot \beta \frac{m_t}{m_T} s_L^u c_L^u e^{i\phi}$

Table XVIII: Light-heavy left couplings of Top quarks to the triplets Higgs $\{h, H, A\}$.

	Y_{htT}^R	Y_{HtT}^R	Y_{AtT}^R
(T)	$(s_{\beta\alpha} + c_{\beta\alpha} \cot \beta) c_L s_L e^{i\phi}$	$(c_{\beta\alpha} - s_{\beta\alpha} \cot \beta) c_L s_L e^{i\phi}$	$-\cot \beta c_L s_L e^{i\phi}$
(XT)	$(s_{\beta\alpha} + c_{\beta\alpha} \cot \beta) \frac{m_t}{m_T} c_R s_R e^{i\phi}$	$(c_{\beta\alpha} - s_{\beta\alpha} \cot \beta) \frac{m_t}{m_T} c_R s_R e^{i\phi}$	$-\cot \beta \frac{m_t}{m_T} c_R s_R e^{i\phi}$
(TB)	$(s_{\beta\alpha} + c_{\beta\alpha} \cot \beta) \frac{m_t}{m_T} s_R^u c_R^u e^{i\phi_u}$	$(c_{\beta\alpha} - s_{\beta\alpha} \cot \beta) \frac{m_t}{m_T} s_R^u c_R^u e^{i\phi_u}$	$-\cot \beta \frac{m_t}{m_T} s_R^u c_R^u e^{i\phi_u}$
(XTB)	$(s_{\beta\alpha} + c_{\beta\alpha} \cot \beta) s_L^u c_L^u e^{i\phi}$	$(c_{\beta\alpha} - s_{\beta\alpha} \cot \beta) s_L^u c_L^u e^{i\phi}$	$-\cot \beta s_L^u c_L^u e^{i\phi}$
(TBY)	$(s_{\beta\alpha} + c_{\beta\alpha} \cot \beta) s_L^u c_L^u e^{i\phi}$	$(c_{\beta\alpha} - s_{\beta\alpha} \cot \beta) s_L^u c_L^u e^{i\phi}$	$-\cot \beta s_L^u c_L^u e^{i\phi}$

Table XIX: Light-heavy right couplings of Top quarks to the triplets Higgs $\{h, H, A\}$.

	Z_{Tb}^L	Z_{Tb}^R
(T)	s_L	$\frac{m_b}{m_T} s_L$
(XT)	0	0
(TB)	$c_L^d s_L^u e^{-i\phi_u} + (s_L^{u2} - s_R^{u2}) \frac{s_L^d}{c_L^d} e^{-i\phi_d}$	$\frac{m_b}{m_T} \left[c_L^d s_L^u e^{-i\phi_u} + (s_R^{d2} - s_L^{d2}) \frac{c_L^d}{s_L^d} e^{-i\phi_d} \right]$
(XTB)	s_L^u	0

Table XX: Heavy-light couplings to the Higgs charged.

References

- [1] **ATLAS** collaboration, *Observation of a new particle in the search for the Standard Model Higgs boson with the ATLAS detector at the LHC*, *Phys. Lett. B* **716** (2012) 1 [[1207.7214](#)].
- [2] **CMS** collaboration, *Observation of a New Boson at a Mass of 125 GeV with the CMS Experiment at the LHC*, *Phys. Lett. B* **716** (2012) 30 [[1207.7235](#)].
- [3] G.C. Branco, P.M. Ferreira, L. Lavoura, M.N. Rebelo, M. Sher and J.P. Silva, *Theory and phenomenology of two-Higgs-doublet models*, *Phys. Rept.* **516** (2012) 1 [[1106.0034](#)].
- [4] R. Benbrik et al., *Signatures of vector-like top partners decaying into new neutral scalar or pseudoscalar bosons*, *JHEP* **05** (2020) 028 [[1907.05929](#)].
- [5] <https://twiki.cern.ch/twiki/bin/view/AtlasPublic>.
- [6] <https://twiki.cern.ch/twiki/bin/view/AtlasPublic/Winter2016-13TeV>.
- [7] <https://twiki.cern.ch/twiki/bin/view/CMSPublic/PhysicsResultsHIG>.
- [8] R. Benbrik, C.-H. Chen and T. Nomura, *Higgs singlet boson as a diphoton resonance in a vectorlike quark model*, *Phys. Rev. D* **93** (2016) 055034 [[1512.06028](#)].
- [9] A. Arhrib, R. Benbrik, S.J.D. King, B. Manaut, S. Moretti and C.S. Un, *Phenomenology of 2HDM with vectorlike quarks*, *Phys. Rev. D* **97** (2018) 095015 [[1607.08517](#)].
- [10] J.A. Aguilar-Saavedra, R. Benbrik, S. Heinemeyer and M. Pérez-Victoria, *Handbook of vectorlike quarks: Mixing and single production*, *Phys. Rev. D* **88** (2013) 094010 [[1306.0572](#)].
- [11] M. Badziak, *Interpreting the 750 GeV diphoton excess in minimal extensions of Two-Higgs-Doublet models*, *Phys. Lett. B* **759** (2016) 464 [[1512.07497](#)].
- [12] A. Angelescu, A. Djouadi and G. Moreau, *Scenarii for interpretations of the LHC diphoton excess: two Higgs doublets and vector-like quarks and leptons*, *Phys. Lett. B* **756** (2016) 126 [[1512.04921](#)].
- [13] J.A. Aguilar-Saavedra, *Identifying top partners at LHC*, *JHEP* **11** (2009) 030 [[0907.3155](#)].
- [14] A. De Simone, O. Matsedonskyi, R. Rattazzi and A. Wulzer, *A First Top Partner Hunter's Guide*, *JHEP* **04** (2013) 004 [[1211.5663](#)].
- [15] S. Kanemura, M. Kikuchi and K. Yagyu, *Fingerprinting the extended Higgs sector using one-loop corrected Higgs boson couplings and future precision measurements*, *Nucl. Phys. B* **896** (2015) 80 [[1502.07716](#)].
- [16] L. Lavoura and J.P. Silva, *The Oblique corrections from vector - like singlet and doublet quarks*, *Phys. Rev. D* **47** (1993) 2046.
- [17] C.-Y. Chen, S. Dawson and E. Furlan, *Vectorlike fermions and Higgs effective field theory revisited*, *Phys. Rev. D* **96** (2017) 015006 [[1703.06134](#)].
- [18] A. Carvalho, S. Moretti, D. O'Brien, L. Panizzi and H. Prager, *Single production of vectorlike quarks with large width at the Large Hadron Collider*, *Phys. Rev. D* **98** (2018) 015029 [[1805.06402](#)].
- [19] S. Moretti, D. O'Brien, L. Panizzi and H. Prager, *Production of extra quarks at the Large Hadron Collider beyond the Narrow Width Approximation*, *Phys. Rev. D* **96** (2017) 075035 [[1603.09237](#)].
- [20] H. Prager, S. Moretti, D. O'Brien and L. Panizzi, *Large width effects in processes of production of extra quarks decaying to Dark Matter at the LHC*, *PoS DIS2017* (2018) 300 [[1706.04007](#)].

- [21] H. Prager, S. Moretti, D. O'Brien and L. Panizzi, *Extra Quarks Decaying to Dark Matter Beyond the Narrow Width Approximation*, in *5th Large Hadron Collider Physics Conference*, 6, 2017 [[1706.04001](#)].
- [22] S. Moretti, D. O'Brien, L. Panizzi and H. Prager, *Production of extra quarks decaying to Dark Matter beyond the Narrow Width Approximation at the LHC*, *Phys. Rev. D* **96** (2017) 035033 [[1705.07675](#)].
- [23] A. Deandrea and A.M. Iyer, *Vectorlike quarks and heavy colored bosons at the LHC*, *Phys. Rev. D* **97** (2018) 055002 [[1710.01515](#)].
- [24] J.A. Aguilar-Saavedra, D.E. López-Fogliani and C. Muñoz, *Novel signatures for vector-like quarks*, *JHEP* **06** (2017) 095 [[1705.02526](#)].
- [25] D. Eriksson, J. Rathsman and O. Stal, *2HDMC: Two-Higgs-Doublet Model Calculator Physics and Manual*, *Comput. Phys. Commun.* **181** (2010) 189 [[0902.0851](#)].
- [26] C. Degrande, C. Duhr, B. Fuks, D. Grellscheid, O. Mattelaer and T. Reiter, *UFO - The Universal FeynRules Output*, *Comput. Phys. Commun.* **183** (2012) 1201 [[1108.2040](#)].
- [27] T. Hahn, *Generating Feynman diagrams and amplitudes with FeynArts 3*, *Comput. Phys. Commun.* **140** (2001) 418 [[hep-ph/0012260](#)].
- [28] J. Kublbeck, M. Bohm and A. Denner, *Feyn Arts: Computer Algebraic Generation of Feynman Graphs and Amplitudes*, *Comput. Phys. Commun.* **60** (1990) 165.
- [29] T. Hahn and C. Schappacher, *The Implementation of the minimal supersymmetric standard model in FeynArts and FormCalc*, *Comput. Phys. Commun.* **143** (2002) 54 [[hep-ph/0105349](#)].
- [30] T. Hahn and M. Perez-Victoria, *Automatized one loop calculations in four-dimensions and D-dimensions*, *Comput. Phys. Commun.* **118** (1999) 153 [[hep-ph/9807565](#)].
- [31] J. Alwall, R. Frederix, S. Frixione, V. Hirschi, F. Maltoni, O. Mattelaer et al., *The automated computation of tree-level and next-to-leading order differential cross sections, and their matching to parton shower simulations*, *JHEP* **07** (2014) 079 [[1405.0301](#)].
- [32] P. Bechtle, O. Brein, S. Heinemeyer, G. Weiglein and K.E. Williams, *HiggsBounds: Confronting Arbitrary Higgs Sectors with Exclusion Bounds from LEP and the Tevatron*, *Comput. Phys. Commun.* **181** (2010) 138 [[0811.4169](#)].
- [33] P. Bechtle, O. Brein, S. Heinemeyer, G. Weiglein and K.E. Williams, *HiggsBounds 2.0.0: Confronting Neutral and Charged Higgs Sector Predictions with Exclusion Bounds from LEP and the Tevatron*, *Comput. Phys. Commun.* **182** (2011) 2605 [[1102.1898](#)].
- [34] P. Bechtle, O. Brein, S. Heinemeyer, O. Stål, T. Stefaniak, G. Weiglein et al., *HiggsBounds – 4: Improved Tests of Extended Higgs Sectors against Exclusion Bounds from LEP, the Tevatron and the LHC*, *Eur. Phys. J. C* **74** (2014) 2693 [[1311.0055](#)].
- [35] P. Bechtle, S. Heinemeyer, O. Stål, T. Stefaniak and G. Weiglein, *Probing the Standard Model with Higgs signal rates from the Tevatron, the LHC and a future ILC*, *JHEP* **11** (2014) 039 [[1403.1582](#)].
- [36] P. Bechtle, S. Heinemeyer, O. Stal, T. Stefaniak and G. Weiglein, *Applying Exclusion Likelihoods from LHC Searches to Extended Higgs Sectors*, *Eur. Phys. J. C* **75** (2015) 421 [[1507.06706](#)].
- [37] P. Bechtle, D. Dercks, S. Heinemeyer, T. Klingl, T. Stefaniak, G. Weiglein et al., *HiggsBounds-5: Testing Higgs Sectors in the LHC 13 TeV Era*, *Eur. Phys. J. C* **80** (2020) 1211 [[2006.06007](#)].

- [38] P. Bechtle, S. Heinemeyer, O. Stål, T. Stefaniak and G. Weiglein, *HiggsSignals: Confronting arbitrary Higgs sectors with measurements at the Tevatron and the LHC*, *Eur. Phys. J. C* **74** (2014) 2711 [[1305.1933](#)].
- [39] P. Bechtle, S. Heinemeyer, T. Klingl, T. Stefaniak, G. Weiglein and J. Wittbrodt, *HiggsSignals-2: Probing new physics with precision Higgs measurements in the LHC 13 TeV era*, *Eur. Phys. J. C* **81** (2021) 145 [[2012.09197](#)].
- [40] H. Bahl, T. Biekötter, S. Heinemeyer, C. Li, S. Paasch, G. Weiglein et al., *HiggsTools: BSM scalar phenomenology with new versions of HiggsBounds and HiggsSignals*, *Comput. Phys. Commun.* **291** (2023) 108803 [[2210.09332](#)].
- [41] F. Mahmoudi, *SuperIso v2.3: A Program for calculating flavor physics observables in Supersymmetry*, *Comput. Phys. Commun.* **180** (2009) 1579 [[0808.3144](#)].
- [42] H. Abouabid, A. Arhrib, R. Benbrik, M. Boukidi and J.E. Falaki, *The oblique parameters in the 2HDM with Vector-Like Quarks: Confronting M_W CDF-II Anomaly*, [2302.07149](#).
- [43] S.-P. He, *Leptoquark and vector-like quark extended model for simultaneous explanation of W boson mass and muon $g-2$ anomalies**, *Chin. Phys. C* **47** (2023) 043102 [[2205.02088](#)].
- [44] J. Cao, L. Meng, L. Shang, S. Wang and B. Yang, *Interpreting the W -mass anomaly in vectorlike quark models*, *Phys. Rev. D* **106** (2022) 055042 [[2204.09477](#)].
- [45] R. Benbrik, M. Boukidi and S. Moretti, *Probing Light Charged Higgs Bosons in the 2-Higgs Doublet Model Type-II with Vector-Like Quarks*, [2211.07259](#).
- [46] **CMS** collaboration, *Search for a vector-like quark $T' \rightarrow tH$ via the diphoton decay mode of the Higgs boson in proton-proton collisions at $\sqrt{s} = 13$ TeV*, *JHEP* **09** (2023) 057 [[2302.12802](#)].
- [47] **ATLAS** collaboration, *Search for charged Higgs bosons decaying into a top-quark and a bottom-quark at $\sqrt{s} = 13$ TeV with the ATLAS detector*, .
- [48] **ATLAS** collaboration, *Search for heavy Higgs bosons decaying into two tau leptons with the ATLAS detector using pp collisions at $\sqrt{s} = 13$ TeV*, *Phys. Rev. Lett.* **125** (2020) 051801 [[2002.12223](#)].